Received: 25 March 2020 | Revised: 21 October 2020 | Accepted: 3 November 2020

DOI: 10.1096/fj.202000704R

RESEARCH ARTICLE

THE FASEB JOURNAL

The phosphatidylinositol transfer protein PITP-1 facilitates fast recovery of eating behavior after hypoxia in the nematode *Caenorhabditis elegans*

Zohar Abergel[1] | **Maayan Shaked**[1] | **Virendra Shukla**[1] | **Zheng-Xing Wu**[2] | **Einav Gross**[1]

[1]Department of Biochemistry and Molecular Biology, Faculty of Medicine, IMRIC, The Hebrew University of Jerusalem, Jerusalem, Israel

[2]Key Laboratory of Molecular Biophysics of Ministry of Education, Department of Biophysics and Molecular Physiology, College of Life Science and Technology, Institute of Biophysics and Biochemistry, Huazhong University of Science and Technology, Wuhan, P.R. China

Correspondence
Zheng-Xing Wu, Key Laboratory of Molecular Biophysics of Ministry of Education, Department of Biophysics and Molecular Physiology, Institute of Biophysics and Biochemistry, College of Life Science and Technology, Huazhong University of Science and Technology, Wuhan, P.R. China.
Email: ibbwuzx@mail.hust.edu.cn

Einav Gross, Department of Biochemistry and Molecular Biology, IMRIC, Faculty of Medicine, The Hebrew University of Jerusalem, PO Box 12271, Jerusalem 9112102, Israel.
Email: einavg@ekmd.huji.ac.il

Funding information
EC | European Research Council (ERC), Grant/Award Number: 281844; Israel Science Foundation (ISF), Grant/Award Number: 989/19

Abstract

Among the fascinating adaptations to limiting oxygen conditions (hypoxia) is the suppression of food intake and weight loss. In humans, this phenomenon is called high-altitude anorexia and is observed in people suffering from acute mountain syndrome. The high-altitude anorexia appears to be conserved in evolution and has been seen in species across the animal kingdom. However, the mechanism underlying the recovery of eating behavior after hypoxia is still not known. Here, we show that the phosphatidylinositol transfer protein PITP-1 is essential for the fast recovery of eating behavior after hypoxia in the nematode *Caenorhabditis elegans*. Unlike the neuroglobin GLB-5 that accelerates the recovery of eating behavior through its function in the oxygen (O_2)-sensing neurons, PITP-1 appears to act downstream, in neurons that express the *mod-1* serotonin receptor. Indeed, *pitp-1* mutants display wild-type-like O_2-evoked-calcium responses in the URX O_2-sensing neuron. Intriguingly, loss-of-function of protein kinase C 1 (PKC-1) rescues *pitp-1* mutants' recovery after hypoxia. Increased diacylglycerol (DAG), which activates PKC-1, attenuates the recovery of wild-type worms. Together, these data suggest that PITP-1 enables rapid recovery of eating behavior after hypoxia by limiting DAG's availability, thereby limiting PKC activity in *mod-1*-expressing neurons.

KEYWORDS

C elegans, GLOBIN 5, hypoxia, oxygen sensing neurons, PITP-1, PKC-1

Abbreviations: AMS, acute mountain syndrome; C, *elegansCaenorhabditis elegans*; DAG, diacylglycerol; GLB, globin; IP_3, inositol 1,4,5-trisphosphate; NPR-1, neuropeptide receptor 1; PITP, phosphatidylinositol transfer protein; PLCβ, phospholipase C beta; PMA, phorbol 12-myristate 13-acetate; PKC-1, protein kinase C 1; PtdIn, phosphatidylinositol; PtdOH, phosphatidic acid; sGC, soluble guanylate cyclases.

Zohar Abergel, Maayan Shaked, and Virendra Shukla contributed equally to the work.

1 | INTRODUCTION

Eating behavior influences our food choice, meal timing, and quantity, and therefore, determines our health and disease state.[1] The factors affecting eating behavior are numerous and diverse and include internal and external cues, one of which being oxygen (O_2). O_2 is essential for energy production in all aerobic animals, and therefore, insufficient O_2 supply (hypoxia) is a significant stress condition in most animals, including humans. Among the fascinating responses to hypoxia is the suppression of food intake and, consequently, body mass loss. This phenomenon is called high-altitude anorexia (or hypoxia-anorexia) and is observed in people suffering from acute mountain syndrome (AMS).[2] AMS occurs in response to a rapid exposure to moderate or high altitudes (above 4000 meters), where the partial O_2 pressure is low. Results from Operation Everest III (Comex-'97) demonstrated that in a controlled environment that mimicked the decrease in O_2 concentration while climbing on Everest at 5000 to 8000 meters, hypoxia was the stimulus that changed the eating behavior of volunteers and decreased food intake due to a loss in appetite.[3] Intriguingly, the hypoxic-anorexia phenomenon appears to be conserved in evolution and has been observed in crabs, flies, gastropods, fish, rodents,[4] and in the nematode *Caenorhabditis elegans* (*C. elegans*).[5,6] The hypoxic-anorexia effect is reversible. Indeed, data from Comex-'97 show that upon returning to ambient O_2-levels, the volunteers' body mass increases.[3] However, the mechanism underlying the recovery of eating behavior after hypoxia is still poorly understood.

The eating behavior of *C. elegans* is modulated by neuronal O_2-sensors and neuropeptide signaling[7,8]. Animals bearing the dominant neuropeptide G-protein-coupled receptor *npr-1(215V)* allele (e.g., N2 laboratory strain) move slowly on bacteria (the *C. elegans* food source) and do not clump together on the bacterial lawn border at 21% O_2[9] By contrast, animals bearing either the recessive *npr-1(215F)* allele (found in many wild *C. elegans* isolates. *e.g*., the Hawaii strain CB4856) or the strong loss-of-function allele *npr-1(ad609)*, hereafter referred to as *npr-1(−)* worms), move fast on food and clump together on the bacterial lawn border (bordering eating behavior) at 21% O_2. The bordering behavior is dependent on the activity of the atypical soluble guanylate cyclases (sGCs) O_2-sensors GCY-35 and GCY-36.[7,8] Upon O_2 binding, the GCY-35/GCY-36 functional complex is thought to generate cGMP that triggers the opening of the TAX-2/TAX-4 cyclic nucleotide-gated channel complex. The opening of TAX-2/TAX-4 facilitates calcium (Ca^{2+}) entry, and thus, the depolarization of the O_2-sensing neurons AQR, PQR, and URX. This cascade activates an escape response from hyperoxia ($O_2 > 12\%$,[10]), which is suppressed by the activity of NPR-1(215V) in the presence of food. Intriguingly, the clumping of worms on the bacteria lawn border appears to decrease the O_2 level that the worm experience. Indeed, a previous study demonstrated that the O_2 level inside the clump ranges between 6.4% and 13.7% O_2,[11] and this is the range of concentrations to which the worm is attracted.[8]

Hypoxia (1% O_2) suppresses the bordering eating behavior and results in worms accumulating outside the bacterial lawn border (Figure 1A). This food-leaving behavior is reversible upon returning to 21% O_2 and is regulated by the neuroglobin GLB-5.[6,10]

Similar to *npr-1*, *glb-5* is a polymorphic gene that affects the worm bordering behavior and foraging speed.[12] In the case of the *npr-1*-gene, N2 worms bear the dominant *npr-1(215V)* gain-of-function allele and the Hawaii strain CB4856 bears the recessive *npr-1(25F)* allele. In contrast, with the *glb-5* gene, N2 worms bear the Bristol allele, hereafter referred to as *glb-5(−)*, which encodes a truncated neuroglobin that appears to be nonfunctional.[13] By contrast, CB4856 worms bear the Hawaii allele of *glb-5*, hereafter referred to as *glb-5(+)*, which encodes a full-length functional neuroglobin that appears to represent the ancestral *glb-5 allele*, as it is found in most *C. elegans* wild-isolates.[13] GLB-5(+) fine-tunes the O_2-responses of worms close to 21% O_2. Indeed, *npr-1(−)* worms that bear the *glb-5(+)* allele (hereafter referred to as *glb-5(+);npr-1(−)* worms) are more sensitive to subtle changes in O_2 level and sharply decrease their foraging speed in response to a 21% to 17% O_2 shift, whereas *npr-1(−)* worms (bearing the *glb-5(−)* allele) display only a mild decrease in response to this stimulus.[13] Like the mammalian cytoglobin[14] and neuroglobin,[15] GLB-5 is a hexacoordinated globin.[16] Hypotheses for hexacoordinated globins' *in vivo* functions include regulation of cellular signaling[13,17,18] and protection against oxidative damage.[19,20]

GLB-5 controls worms' speed and recovery from hypoxia through its activity in the O_2-sensing neurons AQR, PQR, and URX.[13] The recovery of the bordering behavior in *glb-5(+); npr-1(−)* worms, is rapid and occurs within minutes after returning to 21% O_2.[6] By contrast, the recovery of *npr-1(−)* worms bearing the *glb-5(−)* allele is slow and is completed only after 4 hours. This significant difference in recovery time has facilitated the isolation of several suppressor mutations that attenuate bordering behavior recovery by suppressing GLB-5 activity in the O_2-sensing neurons. That is, *glb-5(+); npr-1(−)* animals bearing these mutations do not slowdown in response to a 21% to 17% O_2 shift and display high URX-Ca^{2+} levels at both 14% and 17%% O_2.[6,10] Here, we discover a new type of suppressor mutation in the gene encoding for the phosphatidylinositol (PtdIn) transfer protein PITP-1, which attenuates the recovery of bordering eating behavior without affecting the function of GLB-5 in the O_2-sensing neurons. Our data suggest that PITP-1 facilitates fast recovery of eating behavior after hypoxia by restricting the activation of protein kinase C 1 (PKC-1) by diacylglycerol in *mod-1*-expressing neurons. This function is distinct from the role of PITP-1 in salt chemotaxis.

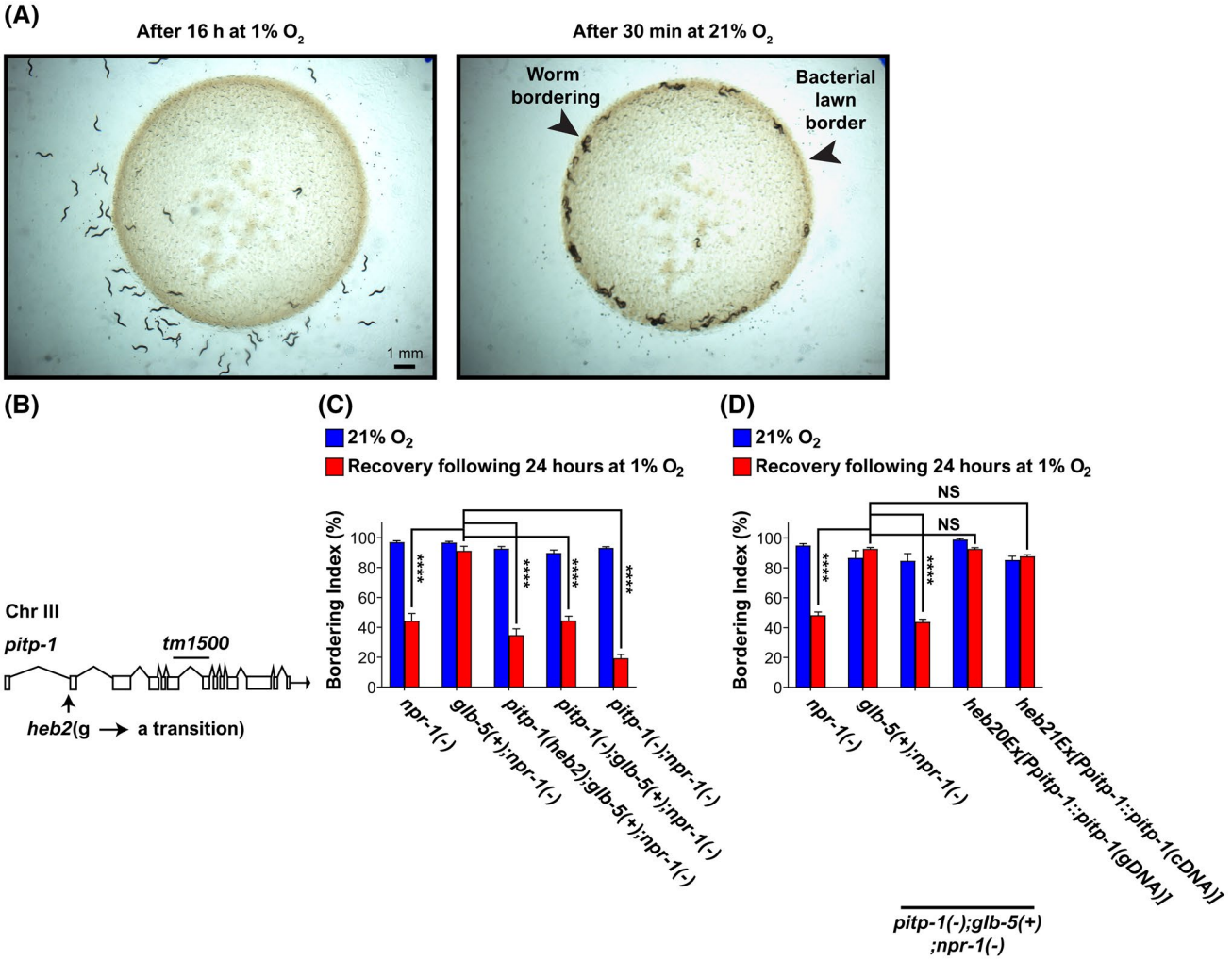

FIGURE 1 PITP-1 is essential for the fast recovery of bordering behavior after hypoxia. A, Hypoxia inhibits the bordering behavior in a reversible way. Left panel, hypoxia-induced food-leaving behavior displayed by *glb-5(+); npr-1(−)* worms after 16 hours incubation in hypoxia (1% O_2). Worms resume robust bordering eating behavior after 30 minutes exposure to 21% O_2 (right panel). In the right panel, the left arrowhead indicates the accumulation of worms on the bacterial lawn border (*i.e.*, bordering). The right arrowhead indicates a region where the bacterial lawn border in readily observed. Scale bar: 1 mm. B, A schematic diagram of the *pitp-1* gene highlighting the splice site mutation in the *heb2* allele. C and D, Bar graphs presenting the recovery of bordering after 24 hours in hypoxia. The bordering index percentage is the fraction of worms located on the bacterial lawn border divided by the total number of worms in the plate, multiplied by 100. Asterisks indicate significance for comparisons with *glb-5(+); npr-1(−)* animals after 24 hours at 1% O_2. Data represent the average of at least six independent experiments. Two-way ANOVA with Bonferroni posttest. ****$P < .0001$, NS, nonsignificant. Error bars represent SEM

2 | MATERIALS AND METHODS

2.1 | Strains

EVG009 *glb-5(Haw) V; npr-1(ad609) X* (the parental strain is AX1891)

EVG034 *npr-1(ad609) X* (the CGC name is DA609)

EVG155 *glb-5 (Bri) V; npr-1(ad609) X; Ex[Pgcy-37::YC2.60 + ccRFP]*

EVG159 *glb-5(Haw) V; npr-1(ad609) X; Ex[Pgcy-37::YC2.60 + ccRFP]*

EVG270 *pitp-1(heb2) III; glb-5(Haw) V; npr-1 (ad609) X*

EVG419, *pitp-1(tm1500) III; glb-5(Haw) V; npr-1(ad609) X; heb21Ex[Ppitp-1::pitp-1(cDNA)::polycismCherry;P-f15e11.1::GFP]*

EVG430 *pitp-1(tm1500) III; glb-5(Haw) V; npr-1(ad609) X; heb20Ex[Ppitp-1::pitp-1(gDNA)::polycismCherry;P-f15e11.1::GFP]*

EVG451 *pitp-1(tm1500) III; glb-5(Haw) V; npr-1(ad609) X; heb22Ex[Pgcy-37::pitp-1(cDNA)::polycismCherry;P-f15e11.1::GFP]*

EVG453 *pitp-1(tm1500) III; glb-5(Haw) V; npr-1(ad609) X; heb23Ex[Pflp-6::pitp-1(cDNA)::polycismCherry;P-f15e11.1::GFP].*

EVG454 *pitp-1(tm1500) III; glb-5(Haw) V; npr-1(ad609) X; heb24Ex[Pglb-5::pitp-1(cDNA)::polycismCherry;Pf15e11.1::GFP]*

EVG511 *pitp-1(tm1500) III; glb-5(Haw) V; npr-1(ad609) X; heb25Ex[Ptax-2::pitp-1(cDNA)::polycismCherry;Pf15e11.1::GFP]*

EVG517 *pitp-1(tm1500)III; glb-5(Haw) V; npr-1(ad609) X; heb26Ex[Pgpa-14::pitp-1(cDNA)::polycismCherry;Pf15e11.1::GFP]*

EVG522 *pitp-1(tm1500) III; glb-5(Haw) V; npr-1(ad609) X; heb28Ex[Pcng-3::pitp-1(cDNA)::polycismCherry;Pf15e11.1::GFP]*

EVG535 *pitp-1(tm1500) III; npr-1(ad609) X*

EVG536 *pitp-1(tm1500) III; glb-5(Haw) V; npr-1(ad609) X; heb29Ex[Pceh-36::pitp-1(cDNA)::polycismCherry;Pf15e11.1::GFP]*

EVG537 *pitp-1(tm1500) III; glb-5(Haw) V; npr-1(ad609) X; heb30Ex[Pocr-2::pitp-1(cDNA)::polycismCherry;Pf15e11.1::GFP]*

EVG542 *pitp-1(tm1500) III; glb-5(Haw) V; npr-1(ad609) X; heb31Ex[Ppitp-1::polycismGFP];Ex[Pglb-5::glb-5::polycismCherry]*

EVG546 *pitp-1(tm1500) III; glb-5(Haw) V; npr-1(ad609) X; heb32Ex[Prgef-1::pitp-1(cDNA)::polycismCherry;Pf15e11.1::GFP]*

EVG577 *pitp-1(tm1500) III; glb-5(Haw) V; npr-1(ad609) X; heb33Ex[Pttx-7::pitp-1(cDNA)::polycismCherry;Pf15e11.1::GFP]*

EVG720 *glb-5(Haw) V; dgk-1(ok1462) npr-1(ad609) X*

EVG800 *pitp-1(tm1500) III; glb-5(Haw) V; dgk-1(ok1462) npr-1(ad609) X*

EVG811 *glb-5(Haw) pkc-1(ok563) V; npr-1(ad609) X*

EVG828 *pitp-1(tm1500) III; glb-5(Haw) pkc-1(ok563) V; npr-1(ad609) X*

EVG875 *pitp-1(tm1500) III; glb-5(Haw) pkc-1(ok563) V; npr-1 (ad609) X; heb34Ex[Pmod-1-1:pkc-1(cDNA)::polycismCherry;Pf15e11.1::GFP]*

EVG877 *pitp-1(tm1500) III; glb-5(Haw) pkc-I(ok563) V; npr-1 (ad609) X; heb35Ex[Prgef-1:pkc-1(cDNA)::polycismCherry;Pf15e11.1::GFP]*

EVG1048 *pitp-1(tm1500) III; glb-5(Haw) V; npr-1 (ad609) X*

EVG1250 *pitp-1(tm1500) III; glb-5(Haw) V; npr-1 (ad609) X; Ex [Pgcy-37::YC2.60 + ccRFP]*

EVG1278 *pitp-1(tm1500) III; glb-5(Haw) V; npr-1(ad609) X; heb39Ex[Pmod-1:pitp-1(cDNA) polycismCherry;Pf15e11.1::GFP]*

EVG1404 *pitp-1(tm 1500) III; glb-5(Haw) pkc-1(ok563) V; npr-1(ad609) X; heb40Ex [Punc-25::pkc-1C::polycismCherry; Pf15e11.1::GFP]*

EVG1407 *glb-5(Haw) V; npr-1(ad609) X; heb41Ex [Pmod-1::pkc-1b(gf)::polycismCherry; Pf15e11.1::GFP].*

EVG1408 *pitp-1(tm 1500) III; glb-5(Haw) V; npr-1(ad609) X; heb42Ex [Punc-25::pitp-1(cDNA) polycismCherry; Pf15e11.1::GFP]*

2.2 | Worm synchronization

To generate synchronized worms, we collected eggs from gravid hermaphrodites using hypochlorite solution.[21] In brief, we collected gravid hermaphrodites into 15 mL tubes by washing the NGM plates three times with M9 buffer (22 mM KH_2PO_4, 42 mM Na_2HPO_4, 86 mM NaCl, and 1 mM $MgSO_4$). We centrifuge the tubes for 1 min (1690 *g*, 1min), and removed the supernatant until 1 mL of volume remained. Then, we added 1 ml of hypochlorite solution (0.5 N NaOH, 1.25% NaOCl) to each tube and inverted it five times. To assist the release of embryos, we aspirated the worm suspensions (back and forth several times) using a syringe with a 21-gauge needle, for 3 minutes. Then, we sedimented the embryos by centrifugation (1690 *g* for 2 minutes) and removed most of the hypochlorite solution. Each tube was washed three times with 5 mL of M9 buffer. Next, we removed most of the M9 buffer (without disturbing the embryos pellet) and added 2 mL of fresh M9 buffer to each tube. We rotated the tubes for 16 hours at room temperature (RT, 21ºC). The hatched L1 larvae were collected by centrifugation (1690 *g* for 3 minutes), counted, and placed into NGM plates seeded with OP50 *E coli* bacteria and grown until the desired developmental stage.

2.3 | Bordering behavior assays

Bordering experiments were performed, as described previously.[10] In brief, 40 L4 hermaphrodites, grown in 21% O_2/21°C, were transferred into a 3.5 cm NGM plate that was seeded 2 days before with 50 µL OP50 bacteria (OD_{600} ~ 0.6). The assay plates were put in 1% O_2 (Coy hypoxia chamber, COY Lab Products Inc, Grass Lake, MI, USA, RT) for 24 hours, and then, brought back to 21% O_2 (control plates were maintained in 21% O_2 at 21°C). We calculated the bordering index (BI) after 30 minutes recovery at 21% O_2. BI (%) represents the fraction of worms found on the bacterial lawn border divided by the total amount of worms on the plate, multiplied by 100%.

2.4 | Speed measurements

All speed measurements were done in the presence of food as described in detail in Abergel et al.[10] In brief, 2 days before the experiment, we put 20 µL OP50 bacteria (OD_{600} ~ 0.6)

on each low-NGM plate (0.13 g/L bacto-peptone) and incubated the plates at RT For each speed experiment, we trapped 8-10 young hermaphrodites inside 500 μm deep rectangular PDMS (12 mm wide, 0.5 mm deep, and 17 mm long). We used a PHD 2000 syringe pump (Harvard Apparatus) to deliver humidified gases to the microfluidic chambers at a flow rate of 0.5 mL/min. We used Teflon valves, controlled by a ValveBank Controller (Automate Scientific), to rapidly switch between different O_2/N_2 gas mixtures. We recorded the movies using a Q-Imaging MicroPublisher 5.0 RTV Microscope Camera (QImaging, RHos) mounted onto an Olympus SZ61 stereomicroscope (Olympus). The videos were taken at 0.5 frames/s. We used custom MATLAB software (The MathWorks)[6] for video analysis. Notably, in our analysis, we did not track worms that leave the bacterial lawn, and thus, only calculated the speed of worms on food.

2.5 | Salt chemotaxis

Salt (NaCl) chemotaxis assays were performed as previously described,[22] with some modifications. In brief, a day before the experiment, we generated a NaCl gradient on a 9-cm chemotaxis assay plate containing 10 mL of 2% agar, 5 mM potassium phosphate (pH 6.0), 1 mM $CaCl_2$, and 1 mM $MgSO_4$. To generate the gradient, we placed a 1.2 cm-diameter agar plug, containing 100 mM of NaCl, 1 centimeter from the edge of the plate. We put one microliter of 0.5 M NaN_3 to the peak of NaCl gradient (the NaCl agar plug) and the equivalent place on the opposite side of the plate. We placed ~200 synchronized young adult hermaphrodites at the center of the assay plate. After 30 minutes, we counted the worms at the NaCl peak and the control spot (1 cm radius from the NaN_3 drop). A chemotaxis index was calculated as followed: [# of animals at the NaCl peak)—(# of animals at the control spot)]/[(total # of animals)—(# of animals at the center of the plate)]. Each data point represents at least six biological repeats.

2.6 | Phorbol 12-myristate 13-acetate treatment

Two days before the experiment, we prepared NGM plates containing 100 μg/mL of ampicillin and 0.1 μg/mL of phorbol 12-myristate 13-acetate (PMA) (dissolved in DMSO, p8139 Sigma Aldrich) or 0.001998% of DMSO as a control. After 24 hours at room temperature (RT), we seeded the plates with 50 μL ampicillin-resistant-OP50 bacteria (OD_{600} ~ 0.6) and let them dry for 24 hours at RT. At the day of the experiment, we placed 40 L4 staged hermaphrodites on the plates and transferred them to 1% O_2 (Coy hypoxia chamber, COY Lab Products Inc, Grass Lake, MI, USA, RT) for 24 hours; control plates remained at 21% O_2. Bordering recovery was measured as described above.

2.7 | Ethyl methanesulfonate mutagenesis screen

The ethyl methanesulfonate (EMS) screen was performed as described in detail in Abergel et al.[10]

2.8 | Mapping

We mapped the *heb2* mutation to a 1.6 Mb genomic interval (on chromosomes III) using SNPs (single nucleotide polymorphisms).[23] The list of additional SNPs primers we used is presented in Table 1. The molecular identity of *heb2* was determined by next-generation sequencing (NGS) at the Technion Genome Center.

2.9 | Molecular biology

Genotyping: The *glb-5(Bri)* duplication was followed by examining the PCR products amplified using primers that flank the duplication in this allele.[13] The *npr-1(215V)* and *npr-1(ad609)* alleles were followed by amplifying the interval containing the mutated allele, and MwoI digestion that distinguishes between the *215V* and *ad609* alleles. The *pitp-1(tm1500)*, *pkc-1 (ok563),* and the *dgk-1(ok1462)* deletion were followed by PCR using primers that flank the deletion region.

2.10 | Transgenes

All rescuing plasmids were generated by either restriction enzyme[24] or Gibson assembly cloning[25] using modified polycistronic mCherry pPD95.75 expression vector, as described previously.[6]

For the *pitp-1(genomic)* rescuing construct *[Ppitp-1::pitp-1(gDNA)::polycismCherry]*, we amplified the *pitp-1* promoter (~4.2 Kb), and genomic region (~8.2 kb) using N2 genomic DNA. The promoter region was amplified with 5′ GTTATCCGCTCCAATCCATCCTTCCAT 3′ and 5′ CCTCTTCTTTTTCGACTCGACAACCCAG 3′ and inserted using BspEI and AvrII. The genomic sequence of *pitp-1* was cloned in two steps. The first genomic part was amplified using 5′ ATGCTGATCAAAGAATACCGTATCCTGTTAC 3′ and 5′ CAGAATTTTGGTACTCACTGTCATCTTG 3′ and inserted using AvrII and PacI. The second part was amplified using 5′ AAAAGTTTGTAAAAACTGATAAAATTTTAGATTCT CCT 3′ and 5′ CTACCGACGATCTTTTTCATTTTCG 3′

TABLE 1 SNP primers, location, band sizes (observed after restriction enzyme digestion) and the respective restriction enzyme. The primer sequences are displayed from 5′ to 3′

Genetic location	Genomic location	Clone	N2 digest	CB4856 digest	Enzyme	Primers
III, -11	2629011-2631354	Y71H2B	355	174, 181	HpyCH4V	F: CCGCGGTGTTCTCTTTGAAATTCTC
						R: GCTCCTTACAGCTTTCAGATCCTC
III, -10.1	2691329-2835114	Y71H2AM	418	27, 124, 267	HphI	F: GATCTGGCAGCTCTGGCGG
						R: GTGCAAGATCCATCGATTCAACG
III, -9	2850762-2893560	F56F11a	251, 304	555	AccI	F: GGGTCACTTGAAAGGTCTTAACAA
						R: TTTCCCGCAATTCGGATGTGTG
III, -8.9	2891762-2892784	F56F11	236, 332	568	AvaII	F: CAGAGCTTCAAGTTTATGGAGGCA
						R: GTACCTCCAAAGTACGCAAACACC
III, -7.9	3052479-3100358	H06I04	513	234, 279	SpeI	F: CTGTAAATCTCAATATCCAAGTGGC
						R: CATGCTTGACTGACCCTAGTTC
III, -6.6	3452186-3486946	C34C12	54, 96, 182	332	NlaIII	F: GCAACCGGTCGCCTTCATAC
						R: TTGTTAACTATGATGCATCGAGGTG
III, -5.4	3558492-3596862	C48G5	641	259, 382	BglII	F: GGGGCTTCTTCATTGCGCTCAC
						R: TTTTCGACGGATCCAGCCATTTCTG
III, -3.8	4112743-4142803	C30D11	117, 473	590	RsaI	F: CATCGAGAAGGACAAGTCGACTA
						R: GGCTCCAAGGCTGCTGCA

inserted using PacI and NotI. To create the *pitp-1* cDNA (~3.1 kb) *[Ppitp-1::pitp-1(cDNA)::polycismCherry]* rescuing construct, the genomic part of the *pitp-1* gene was replaced with *pitp-1* cDNA. The coding region of *pitp-1* was amplified using 5' ATGCTGATCAAAGAATACCGTATCCTGTTAC 3′ and 5′ CTACCGACGATCTTTTTCATTTTCGAATTTTCC 3' and inserted using AvrII and NotI. To express the *pitp-1* cDNA in the oxygen sensing neurons we cut the *gcy-37* and *glb-5* promoters regions from an existing plasmids using BspEI and AvrII, these promoters regions (~1.3 kb, ~3.1 kb, respectively) replace the *pitp-1* promoter, and thus, generate the *[Pgcy-37::pitp-1(cDNA)::polycismCherry]* and *[Pglb-5::pitp-1(cDNA)::polycismCherry]* expression constructs. To express the *pitp-1* cDNA in other specific neurons, we amplified the different promoters using N2 genomic DNA and replaced the promoter region of *pitp-1*. To clone the promoters, we introduced a NgoMIV restriction site to the plasmid backbone (using QuikChange II XL, Agilent Technologies). *flp-6* promoter region (~2.8 kb) was amplified with 5′ CAATTGGATAGGAAATGTCACACGAC 3′ and 5′ ATTCTGGAATAATCATATTGTTTTC 3′ and inserted using NgoMIV and AvrII; *[Pflp-6::pitp-1(cDNA)::polycismCherry]*. *ceh-36* promoter region (~3.1 kb) was amplified with 5′ GAACTCCCGCAGAATGCCAACTTG 3′ and 5′ TGTGCATGCGGGGGCAGGCG 3′ and inserted using NgoMIV and AvrII; *[Pceh-36::pitp-1(cDNA)::polycismCherry]*. *rgef-1* promoter region(~3.6kb) was amplified with 5′ CATCGAATGCAAAAGTCGCAACCTC 3′ and 5′ CGTCGTCGTCGTCGATGCCGTC 3' and inserted using NgoMIV and AvrII; *[Prgef-1::pitp-1(cDNA)::polycismCherry]*. The *tax-2* promoter region (~1.8 kb upstream from ATG+ the first 215 amino acid) was amplified with 5′ CAATGACATCAAACTCGGTCGATGC 3′ and 5′ ATGAAATGTTCCTTTCAATGAAAACCCAAAGC 3′ and inserted using NgoMIV and AvrII; *[Ptax-2::pitp-1(cDNA)::polycismCherry]*. The *ocr-2* promoter region (~3.8kb upstream from ATG+ the first 98 amino acid) was amplified with 5′ GTATGGGAATGTCAGCATGGGAACG 3′ and 5′ CTTTCGTGAGAATGCTCCAAGTCGTTC 3′ and inserted using NgoMIV and AvrII; *[Pocr-2::pitp-1(cDNA)::polycismCherry]*. The *gpa-14* promoter region (~3.3 kb) was amplified with 5' GGTTTCGATGATGTGG TACTTTGGC 3′ and 5′ AAGCTCTCTCAGTTTTGCTT CAAGCTC 3' and inserted using NgoMIV and AvrII; *[Pgpa-14::pitp-1(cDNA)::polycismCherry]*. The *cng-3* promoter region (~760 bp) was amplified with 5′ CACCTCGTGGAATACGGACCTGAAA 3′ and 5′ GTATTG GTGTCAAGAAGGGGGTAG 3′ and inserted using NgoMIV and AvrII; *[Pcng-3::pitp-1(cDNA)::polycismCherry]*. The *mod-1* promoter region (5.5 kb) was cloned in two steps. The first genomic part was amplified using 5′ GTGTTTTCTCGTAATCCCGTTGTACTTCATTG 3′ and 5′ GTCGACAATGCATAAAGGTTCAGTTGCAAG 3′ with SalI restriction enzymes recognize sequence and inserted using NgoMIV and AvrII. The second part was amplified using 5′ ACGTCAAAATCGAATCATTGCTTGGTCTGG 3′ and 5′ AATTTTCTTTCACCGCATTGGCACCTGGAG' inserted using SalI and AvrII; *[Pmod-1:pitp-1(cDNA)polycismCherry]*.

The *ttx-7* promoter region (~0.6 kb) was amplified with 5′ CCAATTGTTAACCTTGAGTATGTCTTCAC 3′ and 5′ CTAAAACTTAAAATCAATGAATAAAGAGCTGAAG 3' and inserted using NgoMIV and AvrII; *[Pttx-7::pitp-1(cDNA)::polycismCherry]*. The constructs were injected into *pitp-1(tm1500);glb-5(Haw);npr-1(ad609)* worms (0.5-2.5 ng/μL) with the PF15E11.1::GFP co-injection marker (47.5-49.5 ng/μL).

For the *pkc-1 cDNA* rescuing constructs, we cut the *pitp-1* cDNA under *rgef-1 and mod-1* promoters with AvrII and NotI and inserted the *pkc-1 cDNA* with AvrII and NotI; *[Prgef-1:pkc-1(cDNA)::polycismCherry]* and *[Pmod-1-1:pkc-1(cDNA)::polycismCherry]*, respectively. The *pkc-1 cDNA* (isoform c) region (~2.3 kb) was amplified with 5′ ATGAAATTCTTCAGTAGTCGGACAATATCATCTG 3′ and 5′ TTAGTAGGTAAAATGCGGATTGATAAATG AAAAACC 3′. The constructs were injected into *pitp-1(tm1500);glb-5(Haw) pkc-1(ok563);npr-1(ad609)* worms (2.5-25 ng/μL) with the PF15E11.1::GFP co-injection marker (25-47.5 ng/μL).

We used Gibson assembly cloning to generate the *[Punc-25::pkc-1C::polycismCherry], [Pmod-1::pkc-1b(gf)::polycismCherry]*, and *[Punc-25::pitp-1 (cDNA) polycismCherry]* expression constructs. The three constructs share the polycistronic mCherry pPD95.75 expression vector that was amplified with 5′ CCACGATGCCTGTAGCAATGGCAAC 3′ and 5′ ATTTCA TTTCCAAGTTGTTAGCGTATCCATCG 3' (~1.6 kb) and with 5′ GTTGCCATTGCTACAGGCATCGTGG 3' and 5' GCTGTCTCATCCTACTTTCACCTAG 3' (~2.8 kb).

For the *[Pmod-1::pkc-1b(gf)::polycismCherry]* rescuing construct, we amplified *mod-1* promoter (~5.5 kb) with 5′ CGATGGATACGCTAACAACTTGGAAATGAAATG TGTTTTCTCGTAATCCCGTTGTACTTC 3′ and 5′ CATATTCATCGTATACCAAACAATCAAAACTCATT ATATTTTAATTTTCTTTCACCGCATTGGCACCTGG 3' and also amplified *pkc-1b* (~1.9 kb[26]) using wild-type N2 cDNA as a template with 5′ CCAGGTGCCAATGCGGTGAAAGAAAATTAAAAT ATAATGAGTTTTGATTGTTTGGTATACGATGAATATG 3′ and 5′ CTAGGTGAAAGTAGGATGAGACAGCGTCG ACTTAGTAGGTAAAATGCGGATTGATAAATGAAA AAC 3′ primer pair. We used Q5 Site-Directed Mutagenesis Kit (NEB) to introduce the A160E gain-of-function mutation into *pkc-1* using 5′ AGACGTGGTGagATGCGACGGA 3′ and 5′ TTGTCGATCATTGAAAGCATTTG 3′ primers. The resulting expression construct was injected into *glb-5 (Haw); npr-1 (ad609)* worms (25-100 ng/μL) with the PF15E11.1::GFP co-injection marker (25-100 ng/μL).

To generate the GABAergic *pitp-1* rescue construct, we amplified the promoter region of *unc-25* (~2 kb) with 5′ cgatggatacgctaacaacttggaaatgaaatCATCATGCCCGCTG CTGTTATCAG 3′ and 5' GTAACAGGATACGGTAT TCTTTGATCAGCATtatattttTTTTGGCGGTGA ACTGAGCTTTTCC 3′ and pitp-1 (~3.1 kb) amplified with 5′ GGAAAAGCTCAGTTCACCGCCAAAAaaaatataA TGCTGATCAAAGAATACCGTATCCTGTTAC 3′ and 5′ ctaggtgaaagtaggatgagacagcgtcgacCTACCGAC-GATCTTTTTCATTTTCGAATTTTCC 3′. This construct was injected into *pitp-1 (tm 1500) III (Haw); npr-1 (ad609)* worms (0.1-1 ng/μL) with the PF15E11.1::GFP co-injection marker (50 ng/μL).

To generate the GABAergic *pkc-1* rescue construct, we amplified the promoter region of *unc-25* (~2 kb) with 5′ cgatggatacgctaacaacttggaaat-gaaatCATCATGCCCGCTGCTGTTATCAG 3′ and 5′ CAGATGATATTGTCCGACTACTGAAGAATTTCATtat atttTTTTGGCGGTGAACTGAGCTTTTCC 3' and also amplified pkc-1c (~2.3 kb) with 5′ GGAAAAGCTCAGTTCACCGCCAAAAaaaatata ATGAAATTCTTCAGTAGTCGGACAATATCATCTG and 5′ ctaggtgaaagtaggatgagacagcgtcgacTTAGTAGGTAAAAT-GCGGATTGATAAATGAAAAACC 3′. The resulted expression construct was injected into *pitp-1 (tm 1500); glb-5 (Haw) pkc-1 (ok653); npr-1 (ad609)* worms (12.5-50 ng/μL) with the PF15E11.1::GFP co-injection marker (12.5-50 ng/μL) (Table 2).

Imaging strains: To image *pitp-1* neurons localization we used the modified plasmid pEnter (95.75 MCS) GFP. We amplified the *pitp-1* promoter (~4.2 Kb) using N2 genomic

TABLE 2 Primers used for deletion strains

	Forward (F) and Reverse (R) sequences
pitp-1(tm1500)	F: CATGGAGATTTCAGCCCGGACAACCC4534
	5105R: GAGATCATACAATAACATCATTTTGCAGGGC
	R: CTGAAAGCTGAGTCTCGATGCTCCAAACTG6033
pkc-1(ok563)	F: GACTCGGCGTTGATTAATGAGCTTTCTCG
	F1: GACCTGAAAGGATAGAAATGGTGATTGGCTTG
	R: GATCAAACGCTATTCGGGTATTCGCAACG
dgk-1(ok1462)	F: CCTCCGGATTATTCATCGTCTGTTCG
	R: GACGTTGAACCACTCCTTGTGCTAG
	R1: CTATGGCGAGAAGTCACACCACATTG

DNA. The promoter was inserted with NheI and XbaI. The constructs were injected into *pitp-1(tm1500);glb-5(Haw);npr-1(ad609)* worms. To validate the expression of *pitp-1* in the O_2-sensing neurons, we crossed this strain with the AX1846 strain, which expressed mCherry under the promoter region of *glb-5*.[13] The Ca^{2+} imaging strains were generated as described previously.[6,10] The *Pgcy-37::YC2.60* extrachromosomal array was introduced to *pitp-1(tm1500);glb-5(Haw);npr-1(ad609)* worms by crossing with the EVG159 parental strain.[10]

2.11 | Ca^{2+} imaging

We performed the Ca^{2+} imaging experiments as described in.[10] We recorded the Ca^{2+} responses at two frames per second, using an Olympus IX71S1F-3-5 inverted microscope equipped with UAPON40X Universal apochromatic water immersion objective (Olympus, Tokyo, Japan), DV2 2-channel imager (Photometrics), Rolera EM-C2 (Qimaging), and MetaMorph software (Molecular Devices). To immobilize worms, we glued them to agarose pads (2% agarose in M9) using Dermabond topical skin adhesive (Ethicon). These worms were trapped inside a 500 μm deep rectangular PDMS chamber (12 mm wide, 0.5 mm deep, and 17 mm long). In all of our imaging experiments, humidified gases were delivered to the microfluidic chambers using a PHD 2000 syringe pump (Harvard Apparatus, Holliston, MA, United States) at a flow rate of 0.5 ml per minute. Teflon valves, regulated by a ValveBank Controller (Automate Scientific, Berkeley, California, USA), were used to rapidly switch between gas mixtures. Image analysis was performed using custom-written MATLAB software.

2.12 | Aldicarb assays

We adapted the aldicarb assay protocol described in.[26] In brief, a day before the experiment, we prepared experimental NGM plates containing 1.5 mM of aldicarb (33386-100MG Sigma Aldrich; stock solution: 50 mM in 70% ethanol). After 5 hours at RT, we seeded the plates with 100 μL of OP50 bacteria (OD_{600} ~ 0.6) and let them dry for 24 hours at RT. On these plates, we placed young adult hermaphrodites that were either exposed to hypoxia (1% O_2) for 24 hours as described above or remained at 21% O_2. We measured paralysis every 20 minutes for 2 hours. Paralysis is defined by the absence of movement when poked three times with an eyelash on the head and tail. The 1% and 21% O_2-aldicarb assays included five biological replicates, in which at least 120 worms were examined.

2.13 | Statistical analysis

For comparison between two groups, we used an unpaired t test with Welch's correction. For comparison between more than two groups, when two parameters are explored (ie, the effect of O_2 level and genetic background), we used two-way ANOVA with Bonferroni posttest. For the aldicarb assays, we used the log-rank (Mantel-Cox) test. Data are presented as mean ± SEM (standard error of the mean) or as a Kaplan-Meier curve (ie, in the case of the aldicarb experiments). All statistical analysis was performed using GraphPad Prism version 8.0.0 for Windows, GraphPad Software, San Diego, California USA, www.graphpad.com.

3 | RESULTS

3.1 | PITP-1 is required for fast recovery of the bordering eating behavior after hypoxia

GLB-5 accelerates the rate of bordering feeding behavior recovery after hypoxia.[6,10] To explore the underlying mechanism, we performed an EMS mutagenesis screen and isolated *glb-5(+); npr-1(−)* mutants that fail to display wild-type bordering behavior (after 24 hours exposure at 1% O_2, followed by 30 min recovery at 21% O_2). To avoid isolating mutants that are generally defective in their O_2-sensing and/or bordering behavior, we verified that these mutants resume wild-type bordering behavior after 4 hours recovery at 21% O_2. We used single nucleotide polymorphism (SNP) mapping[23] to locate one of these mutations, *heb2*, to a 1.6 Mb genomic interval on chromosome III. By whole-genome sequencing (Illumina), we identified 10 point mutations in this genomic region. Among these mutations, a G > A transition mutation disrupts a splice-acceptor site in the *pitp-1* gene (Figure 1B). *pitp-1* encodes the sole class IIA phosphatidylinositol transfer protein (PITP) in *C elegans*,[27] sharing high sequence similarity with the human Nir2 protein.[28] To confirm the *pitp-1(heb2)* phenotype, we tested the bordering recovery of a *pitp-1* deletion mutant, that is, *pitp-1(tm1500)*,[27] which lacks approximately 950 bp from the *pitp-1* genomic region. The bordering behavior of *pitp-1(heb2)* and *pitp-1(tm1500)* mutants was similar (Figure 1C), suggesting that *pitp-1(heb2)* is nonfunctional. Since tracking the *tm1500* allele is easier than *heb2*, we have continued working with *pitp-1(tm1500)* allele (hereafter referred to as *pitp-1(−)*). Finally, we confirmed the necessity of *pitp-1* to the rapid recovery of bordering behavior by generating transgenic *pitp-1(−); glb-5(+); npr-1(−)* worms that express either the genomic or coding region of *pitp-1* under its promoter region (Figure 1D).

3.2 | PITP-1 is not generally required for GLB-5-dependent O_2 responses

So far, all the characterized GLB-5 suppressors have been found to affect the O_2-sensing pathway in the AQR, PQR, and URX neurons. This occurs by directly changing the function of the O_2-sensors GCY-35 and GCY-36[10] or by interfering with their transport to the dendritic endings of URX.[6] To explore the mechanism by which PITP-1 regulates GLB-5 activity, we first set out to determine whether it is co-expressed with *glb-5* in the AQR, PQR, and URX neurons. For this, we generated transgenic worms co-expressing a GFP and a mCherry fluorescent tags under the promoter regions of *pitp-1* and *glb-5*, respectively. As previously reported, *pitp-1* is expressed in many neurons.[27] We observed a co-localization of the GFP and mCherry fluorescence in the AQR, PQR, and URX neurons (Figure 2A), as well as in the BAG O_2-sensing neurons (the BAG neurons act reciprocally to the URX neurons and are activated at low O_2 levels[29]), indicating that *pitp-1* is co-expressed with *glb-5* in O_2-sensing neurons.

Next, we asked whether *pitp-1* activity in these neurons is sufficient to rescue the fast bordering recovery after hypoxia. To answer this, we generated two transgenic *pitp-1(−); glb-5(+); npr-1(−)* worm strains expressing the coding region of *pitp-1* just in AQR, PQR, and URXL/R (under the promoter region of *gcy-37*) or in all six O_2-sensing neurons (*i.e.*, URX L/R, AQR, PQR, and BAG L/R) under the promoter region of *glb-5*.[13,30] The expression of *pitp-1*, either in the four or the six neurons, did not restore fast bordering after hypoxia (Figure 2B), suggesting the *pitp-1* acts in other neurons to accelerate the recovery of feeding behavior after hypoxia.

To further explore *pitp-1* function, we asked whether it is generally important for *glb-5* activity. To explore this, we performed speed assay experiments in which we exposed *npr-1(−)*, *glb-5(+); npr-1(−)*, and *pitp-1(−); glb-5(+); npr-1(−)* worms to a 21%-17% O_2 shift. We use this O_2 shift as an indicator for *glb-5* activity because it induces a significant decrease in the foraging speed of *glb-5(+); npr-1(−)* worms, however, only a mild decrease in *npr-1(−)* worms that bear a nonactive *glb-5*.[10,13] As expected, the shift from 21% to 17% O_2 induced a robust decrease in the speed of *glb-5(+); npr-1(−)* worms, and a mild decrease in *npr-1(−)* worms (Figure 2C). The speed-shift observed in *pitp-1(−); glb-5(+); npr-1(−)* worms was similar to that seen in *glb-5(+); npr-1(−)* controls, suggesting that *pitp-1* is not required for *glb-5* activity in this behavioral paradigm.

3.3 | O_2-evoked Ca^{2+} responses in URX in *pitp-1* mutants

To directly explore whether *pitp-1* is important for *glb-5*-mediated O_2 responses, we performed Ca^{2+} imaging experiments. For this, we expressed the ratiometric YC2.60 Ca^{2+} sensor in the URX neurons (as described in[10]) of *npr-1(−)*, *glb-5(+);npr-1(−)*, and *pitp-1(−); glb-5(+); npr-1(−)* worms. These worm strains were exposed to 1% O_2 for 24 hours or remained at 21% O_2 as a control (*i.e.*, naïve worms). We chose the 21% to 14% shift because it mimics the O_2-concentration change that the worms experience when entering the bacterial lawn border, where the O_2 level is lower than the lawn center and its surroundings.[8] The 21% to 14% O_2 shift elicited a significant drop in Ca^{2+} concentration in naïve worms of the three strains (Figure 3A-C). After 24 hours exposure to hypoxia, the 21%-14% O_2 shift did not induce a Ca^{2+} drop in *npr-1* worms (Figure 3A). This result is in line with previous studies that show that a functional *glb-5* is essential for decreasing the sensitivity of the URX neurons after exposure to hypoxia.[10] By contrast, the shift from 21% to 14% O_2 induced a significant decrease in the Ca^{2+} level of both *glb-5(+); npr-1(−)* and *pitp-1(−); glb-5(+); npr-1(−)* worms (Figure 3B,C). The magnitude of the Ca^{2+} drop was similar between the two strains. Together, these results suggest that *pitp-1* is not required for *glb-5*-dependent O_2 responses in the O_2-sensing neurons.

3.4 | PITP-1 roles in salt/benzaldehyde chemotaxis and recovery from hypoxia are distinct

Where does PITP-1 act to facilitate fast recovery from hypoxia? A previous study by Iino and colleagues showed that PITP-1 acts in the ASEL/R neurons to regulate salt (NaCl) chemotaxis/chemorepulsion and in the AWC and the ASH neurons to promote, respectively, olfaction and osmotic avoidance.[27] Therefore, we explored whether *pitp-1* acts in the ASE and the AWC neurons to facilitate fast recovery from hypoxia. We generated transgenic *pitp-1(-); glb-5(+); npr-1(-)* worms expressing *pitp-1* under the *flp-6* promoter region (ASE neurons[31]) or under the *ceh-36* promoter region (ASE and AWC neurons[32]). Expression of *pitp-1* in just the ASE or the ASE/AWC neurons did not rescue the fast recovery of bordering behavior after 24 hours exposure to hypoxia (Figure 4A). By contrast, the expression of *pitp-1* in these neurons (just in ASE or in both ASE and AWC) restored the chemotaxis attraction to salt (Figure 4B), albeit to a lower level than wild type. Together, these results indicate that the place of activity of PITP-1 in the control of salt chemotaxis is different from the place of its activity in the regulation of feeding behavior after hypoxia.

3.5 | PITP-1 acts in MOD-1-expressing neurons to promote fast recovery from hypoxia

To determine where *pitp-1* activity is required for the fast bordering recovery after hypoxia, we restricted the expression

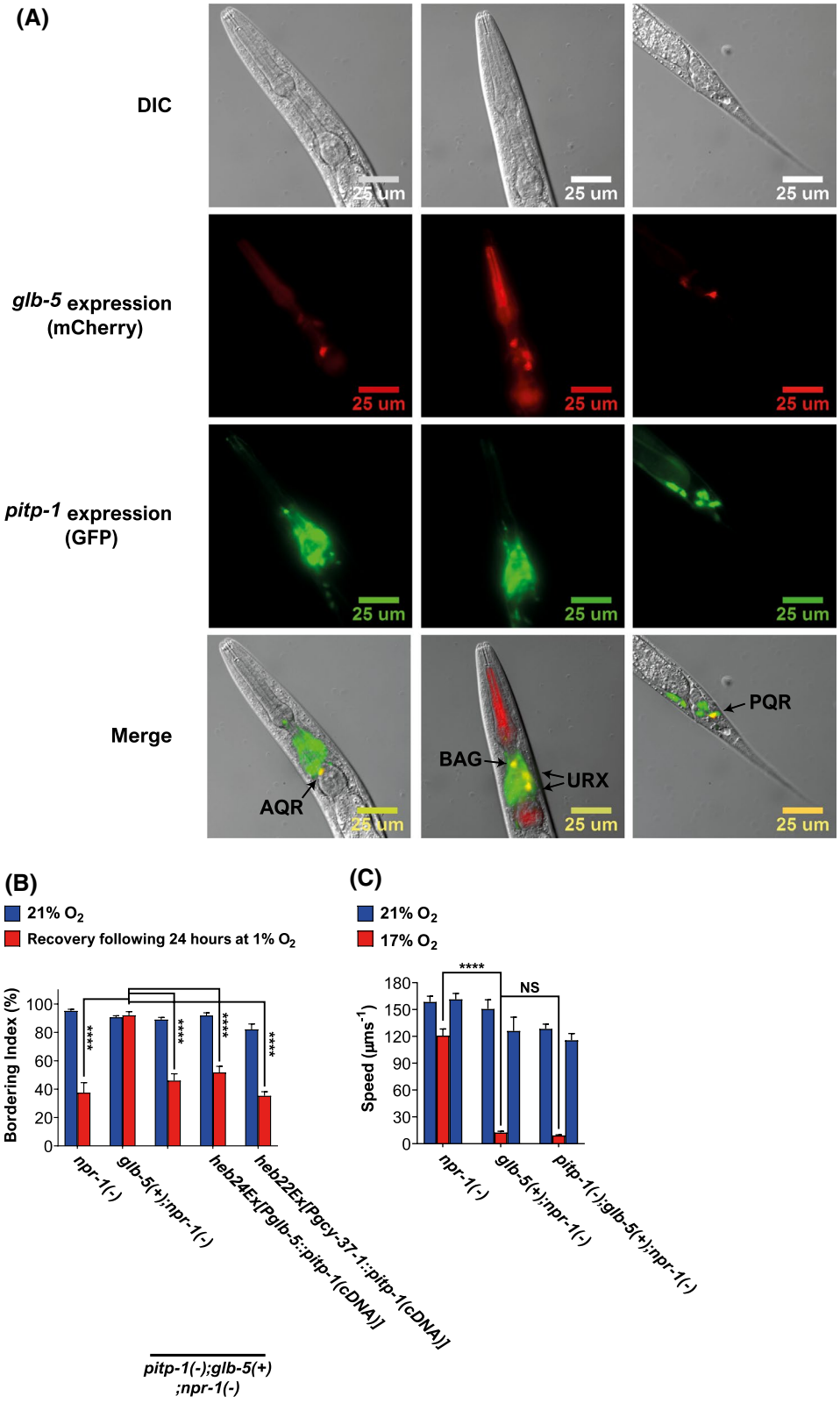

FIGURE 2 Expression of *pitp-1* in the O_2-sensing neurons AQR, PQR, URX, and BAG does not rescue the fast recovery of bordering behavior after hypoxia. A, Bright-field and fluorescence images of transgenic worms co-expressing *Pglb-5::glb-5::mCherry* and *Ppitp-1::pitp-1::GFP*. Arrows indicate the AQR, BAG, PQR, and URX neurons in the merge images. Scale bars: 25 μm. B, A bar graph presenting the recovery of bordering after 24 hours in hypoxia. Asterisks indicate significance for comparisons with *glb-5(+); npr-1(−)* animals after 24 hours at 1% O_2. C, Speed measurements. The speed of worms was measured at 21% and 17% O_2 in the presence of bacteria. Asterisks indicate significance for comparisons with *glb-5(+); npr-1(−)* worm speed at 17% O_2. Data represent the average of at least six independent experiments. Two-way ANOVA with Bonferroni posttest. ****$P < .0001$, NS, nonsignificant. Error bars represent SEM

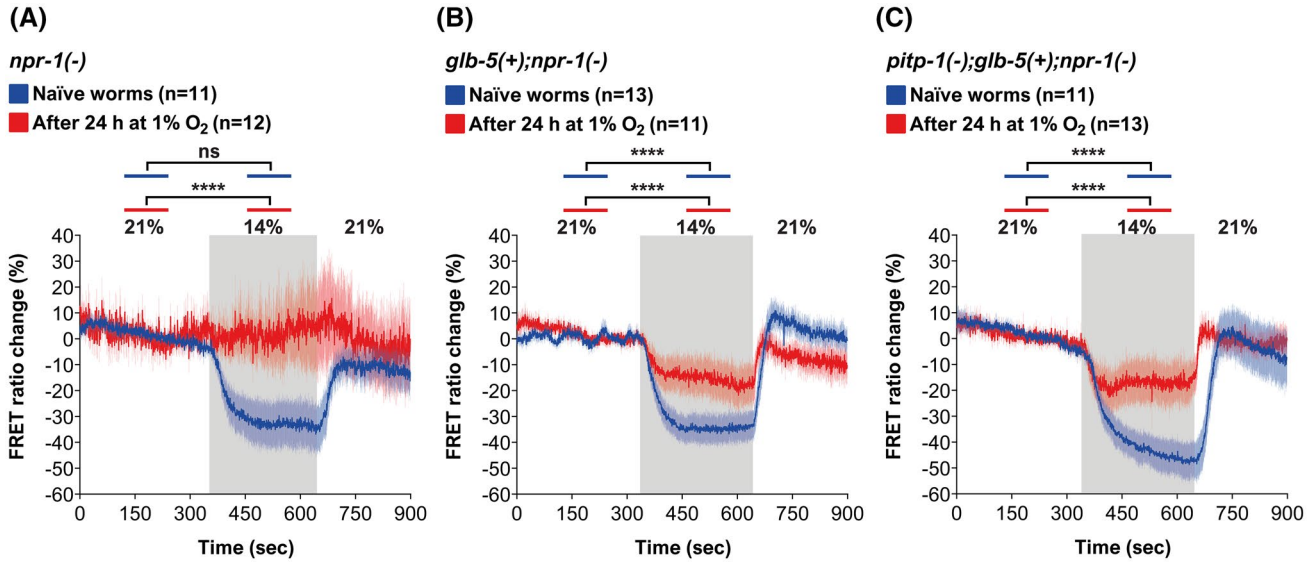

FIGURE 3 PITP-1 is not required for *glb-5*-dependent O_2 responses in the URX neurons. A-C, Ca^{2+} imaging in animals expressing the Cameleon YC2.60 in the URX neurons. The responses were measured in naïve worms (grown in 21% O_2, blue Ca^{2+} traces) or in worms exposed to 1% O_2 (red Ca^{2+} traces). Asterisks indicate significant differences at times specified by bars between the Ca^{2+} levels, unpaired t test with Welch's correction. Gray shading indicates 14% O_2. n = the number of worms imaged in each strain. Error bars (lighter shading) represent SEM

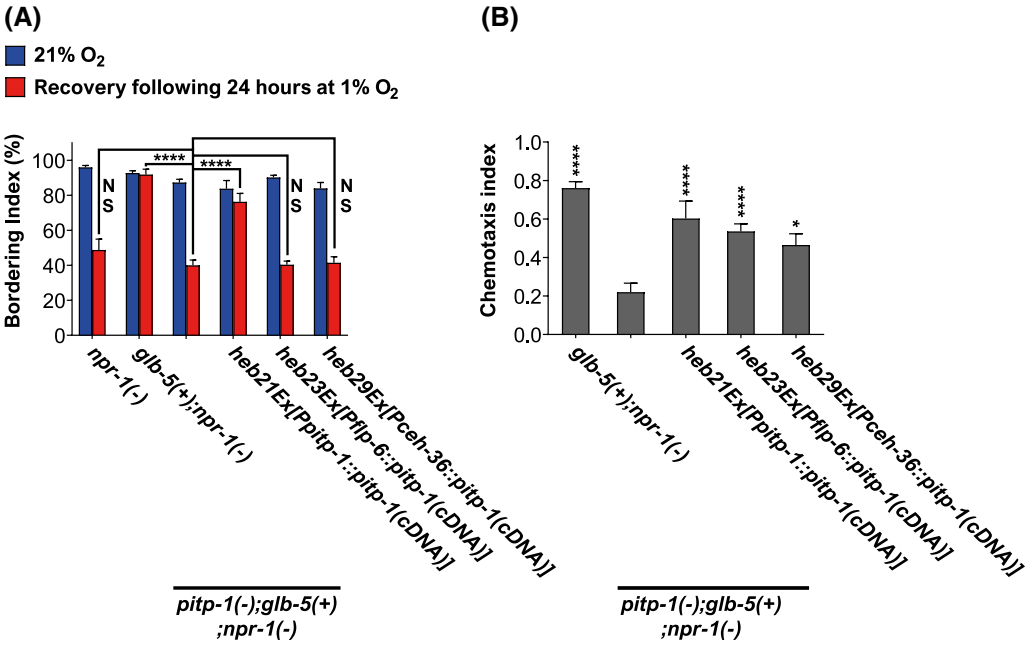

FIGURE 4 PITP-1 functions in salt chemotaxis and recovery from hypoxia are distinct. A, A bar graph presenting the recovery of bordering after 24 hours in hypoxia. Asterisks indicate significance for comparisons with *pitp-1(−); glb-5(+); npr-1(−)* worms after 24 hours at 1% O_2. B, Bar graph showing the attraction of worms to sodium chloride (NaCl). Asterisks indicate significance for comparisons with *pitp-1(−); glb-5(+); npr-1(−)* worms. Data represent the average of at least six independent experiments. Two-way ANOVA with Bonferroni posttest. *$P < .05$, ****$P < .0001$. Error bars represent SEM

of *pitp-1* cDNA to a subset of neurons using the following promoters: *cng-3* [AFD, ASE, ASI, AWB, and AWC[33]], *gpa-14* [ADE, ALA, ASH, ASI, ASJ, ASK, AVA, CAN, DVA, PHA, PHB, PVQ, and RIA[34]], *mod-1* [AIA, AIB, AIY, AIZ, DD, RIC, RID, RIM, RME, and VD[35-37]], *ocr-2* [expressed in PHA, PHB, ASH, ADL, ADF and AWA[38,39]], *tax-2* [expressed in the AWC, AFD, ASE, ASG, ASJ, AQR, BAG, ASK, ASI, AWB, and PQR neurons[40,41]], and *ttx-7* [ADF,

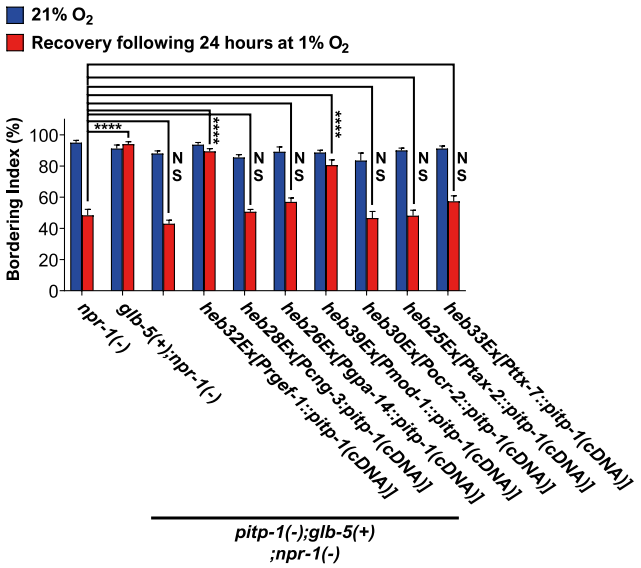

FIGURE 5 Expression of *pitp-1* under the promoter region of *mod-1* rescues the fast recovery of bordering behavior after hypoxia. A bar graph presenting the recovery of bordering after 24 hours in hypoxia in transgenic *pitp-1(−); glb-5(+); npr-1(−)* worms expressing wild-type *pitp-1*(cDNA) under different neuron promoter regions. Asterisks indicate significance for comparisons with *npr-1(−)* animals after 24 hours at 1% O_2. Data represent the average of at least six independent experiments. Two-way ANOVA with Bonferroni posttest. ****$P < .0001$, NS, nonsignificant. Error bars represent SEM

ADL, AFD, ASE, ASH, ASI, ASJ, ASK, AWB, AWC, RIA, and VNC[42]]. In addition, we used the *rgef-1* promoter to express *pitp-1* in all neurons[43] as a positive control. As expected, transgenic *pitp-1(−); glb-5(+); npr-1(−)* worms expressing *pitp-1* under the *rgef-1* promoter region showed full rescue of bordering behavior after hypoxia (Figure 5). Intriguingly, the expression of *pitp-1* under the *mod-1* promoter region resulted in a significant rescue of the bordering behavior after hypoxia, albeit to a lesser degree than the *rgef-1* promoter (Figure 5). These results suggest that PITP-1 acts in *mod-1*-expressing neurons to regulate the recovery of feeding behavior after hypoxia.

GABAergic neurons appear to be involved in neuronal response to hypoxia[44] and food-sensing in *C elegans*.[45] Since the *mod-1*-expressing neurons DD, RME, and VD are GABAergic,[46] we asked whether PITP-1 acts in these neurons to facilitate fast bordering recovery after hypoxia. To explore this, we expressed *pitp-1* under the GABAergic-specific promoter *unc-25*.[47] in *pitp-1(−); glb-5(+); npr-1(−)* worms and examined the recovery of bordering after hypoxia. The bordering recovery of transgenic GABAergic::*pitp-1* worms was similar to *pitp-1(−); glb-5(+); npr-1(−)* mutants (Figure S1A), suggesting that PITP-1 function in these GABAergic neurons is not sufficient to facilitate fast bordering recovery after hypoxia.

3.6 | Impairment of PKC-1 activity restores rapid bordering recovery after hypoxia in *pitp-1* mutants

A previous study showed that the function of PITP-1 in salt chemotaxis plasticity is mediated, in part, by diacylglycerol (DAG) signaling.[27] A key target of DAG is the protein kinase C 1 (PKC-1), which is predicted to require DAG for activation.[48-50] To explore the function of PKC-1 in the PITP-1-dependent recovery from hypoxia, we first asked whether PKC-1 itself is required for the fast recovery. To answer this, we generated *glb-5(+); npr-1(−)* worms bearing the *pkc-1(ok563)* deletion allele (hereafter referred to as *pkc-1(−)*), which removes ~1.3 Kb from the 5′ UTR of the *pkc-1B* splice isoform (including the ATG translation initiation site).[50] The bordering recovery of *glb-5(+) pkc-1(−); npr-1(−)* worms from hypoxia was similar to *glb-5(+); npr-1(−)* controls ($P > .9999$; Figure 6A), indicating that PKC-1 is not required for the fast recovery of bordering behavior. We next introduced *pkc-1(ok563)* into *pitp-1(−); glb-5(+); npr-1(−)* worms and examined their bordering recovery after hypoxia. Intriguingly, *pkc-1* loss-of-function rescued the fast bordering recovery after hypoxia (Figure 6A), albeit to a lesser degree in comparison to *glb-5(+); npr-1(−)* controls. This result suggests that PKC-1 activity inhibits the fast recovery from hypoxia in *pitp-1(−); glb-5(+); npr-1(−)* worms.

PITP-1 controls the recovery from hypoxia through its activity in *mod-1*-expressing neurons (Figure 5). Therefore, we asked whether *pkc-1* acts in these neurons to inhibit the fast bordering recovery of *pitp-1(−);glb-5(+) pkc-1(−); npr-1(−)* worms after hypoxia. To explore this, we generated transgenic *pitp-1(−); glb-5(+) pkc-1(−); npr-1(−)* worms expressing *pkc-1(wt)* under the promoter region of *mod-1*. Moreover, we generated two additional rescuing strains. One expresses *pkc-1(wt)* in all neurons, under the promoter region of *rgef-1*, and thus, serves as a positive control for neuronal *pkc-1* activity. The second expresses *pkc-1(wt)* just in GABAergic neurons, under the promoter region of *unc-25*. Expression of *pkc-1(wt)* in all neurons or only in the *mod-1*-expressing neurons resulted in a significant and a similar degree of bordering-inhibition ($P_{Prgef\text{-}1\ vs\ Pmod} = .6755$), suggesting that no other neurons, besides the *mod-1*-neurons, are important for this inhibitory activity of PKC-1. Unexpectedly, restoring PKC-1 activity under the *unc-25* promoter resulted in a small, yet, a significant decrease in the recovery of bordering after hypoxia (Figure S1B), suggesting that the activity of PKC-1 in one or more of the GABAergic neurons DD, RME, and VD contributes to the inhibition of bordering after hypoxia. Together, these results indicate that PKC-1 activity in the *mod-1*-expressing neurons decreases bordering recovery after hypoxia. Furthermore, they suggest that the function of PITP-1 is to attenuate PKC-1 activity in these neurons. Finally, although *pitp-1* expression in DD, RME, and VD is not sufficient for rescuing the fast recovery of bordering

after hypoxia, the above *pkc-1*-rescuing experiments suggest that one or more of these neurons play a role in the recovery of bordering after hypoxia.

To further explore PKC-1 function, we asked whether constitutive PKC-1 activity in the *mod-1*-expressing neurons would interfere with the recovery of bordering after hypoxia. For this, we overexpressed a gain of function mutation of *pkc-1* in the *mod-1*-expressing neurons of *glb-5(+); npr-1(−)* worms. This *pkc-1* mutation, hereafter referred to as *pkc-1(gf)*, substitutes alanine 160 for glutamate in the pseudosubstrate domain of

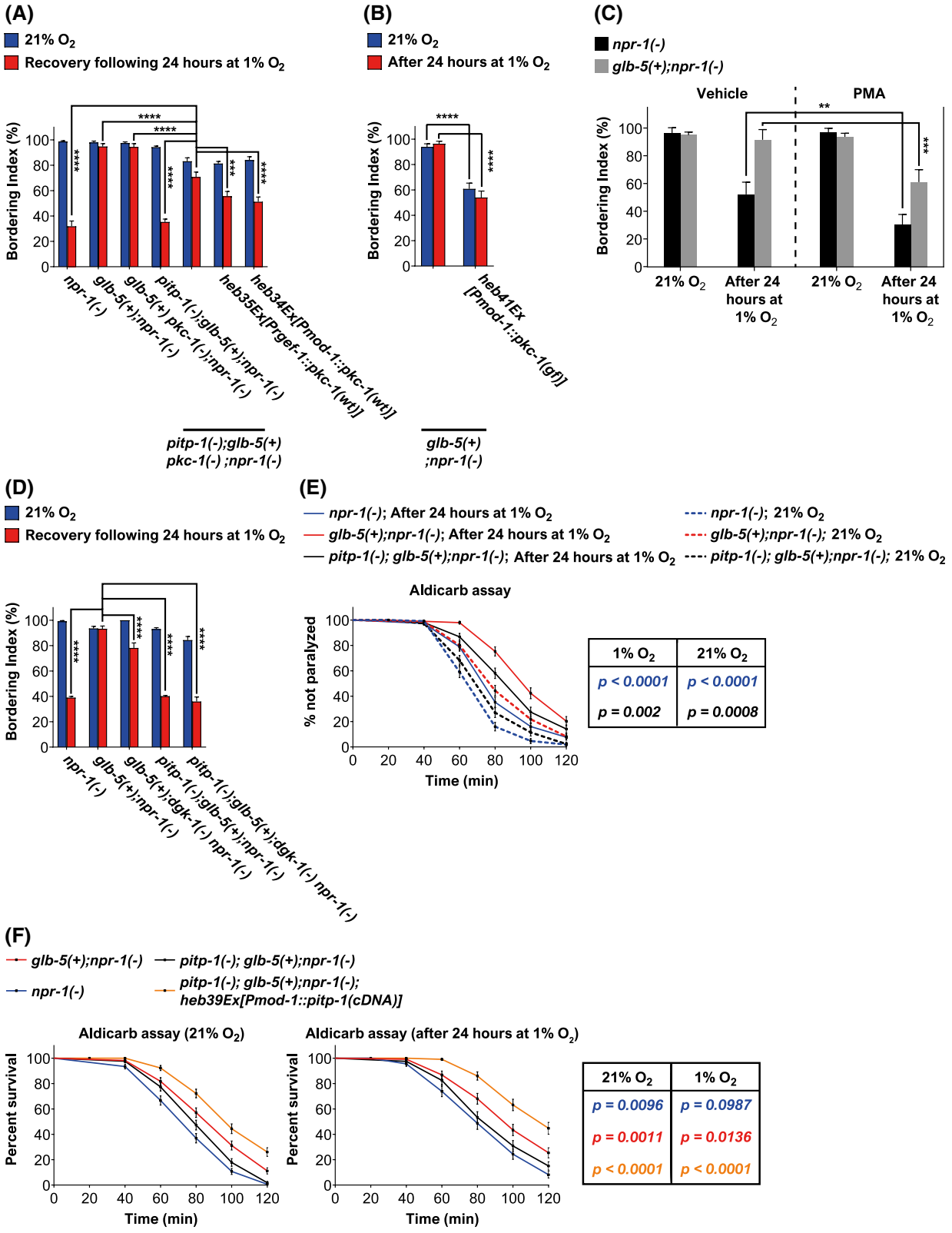

FIGURE 6 PKC-1 loss of function enhances the bordering recovery of *pitp-1(−); glb-5(+); npr-1(−)* worms after hypoxia. A-D, Bar graphs presenting the recovery of bordering after 24 hours in hypoxia. In (A), asterisks indicate significance for comparisons with *pitp-1(−); glb-5(+) pkc-1(−); npr-1(−)* worms after 24 hours at 1% O_2. In (C), significance was calculated in PMA-treated animals, each strain compared to the 21% O_2 controls. In (D), asterisks indicate significance for comparisons with *glb-5(+); npr-1(−)* worms after 24 hours at 1% O_2. All bordering experiments represent at least six biological repeats. For (A), (B), and (D), we used two-way ANOVA with Bonferroni posttest. For (C), we used multiple t tests with Holm-Sidak multiple comparison correction. $^{**}P < 0.01$, $^{***}P < .001$, $^{****}P < .0001$, NS, nonsignificant. Error bars represent SEM. E and F, Aldicarb paralysis assays. E, Aldicarb response of *npr-1(−)*, *glb-5(+), npr-1(−)*, and *pitp-1(−); glb-5(+); npr-1(−)* worms after exposure to 1% O_2 (24 hours) or 21% O_2 (control). Inset table, *p* values indicate significance for comparisons with *glb-5(+); npr-1(−)* worms at 1% and 21% O_2; the *npr-1(−)/glb-5(+); npr-1(−)* comparison in blue, the *glb-5(+); npr-1(−)/pitp-1(−); glb-5(+); npr-1(−)* comparison in black. F, In addition to the strains explored in (E), we investigated the response of transgenic *pitp-1(−); glb-5(+); npr-1(−); heb39Ex[Pmod-1::pitp-1(cDNA)]* worms to aldicarb. Inset table, *P* values indicate significance for comparisons with *pitp-1(−); glb-5(+); npr-1(−)* worms at 1% and 21% O_2; the *npr-1(−)/pitp-1(−); glb-5(+); npr-1(−)* comparison in blue, the *glb-5(+); npr-1(−)/pitp-1(−); glb-5(+); npr-1(−)* comparison in red, and the *pitp-1(−); glb-5(+); npr-1(−); heb39Ex/pitp-1(−); glb-5(+); npr-1(−)* comparison in orange. Log-rank (Mantel-Cox) test. The aldicarb experiments represents five biological repeats

PKC-1, resulting in constitutive enzymatic activity.[51] The bordering index of transgenic *pkc-1(gf)* worms after hypoxia was significantly lower compared to the parental *glb-5(+);npr-1(−)* worms (~54% compared to ~96%, after hypoxia, Figure 6B). In fact, the bordering index of transgenic *pkc-1(gf)* worms was low even in control worms that did not experience hypoxia, indicating that constitutive PKC-1 activity in the *mod-1*-expressing neurons inhibits the bordering behavior of *glb-5(+);npr-1(−)* worms irrespective of the exposure to hypoxia. These data support the hypothesis that excessive PKC-1 activity in the *mod-1*-expressing neurons suppresses bordering after hypoxia.

3.7 | PMA inhibits fast recovery of bordering behavior after hypoxia

How does PITP-1 attenuate PKC-1 activity? Since PKC-1 is thought to be activated by DAG.[51] and PITP-1 can potentially affect the level of DAG,[28], we hypothesized that excess of DAG would attenuate the recovery of bordering behavior of *glb-5(+); npr-1(−)* worms. To test this, we put *glb-5(+); npr-1(−)* and *npr-1(−)* worms on NGM-plates containing PMA, a DAG analog that binds and activates PKC,[50] and measured the recovery of bordering behavior after hypoxia. In addition, we measured the effect of PMA on the bordering behavior of control worms that were not exposed to hypoxia and in worms exposed to 0.002% DMSO (the PMA vehicle). PMA significantly decreased the bordering recovery of both *glb-5(+); npr-1(−)* and *npr-1(−)* worms after hypoxia (Figure 6C); however, it did not affect the bordering behavior of control worms.

To further explore whether increased DAG signaling can inhibit the recovery of bordering behavior after hypoxia, we introduced the *dgk-1(ok1462)* null mutation (hereafter referred to as *dgk-1(−)*) into the genetic background of both *glb-5(+); npr-1(−)* and *pitp-1(−); glb-5(+); npr-1(−)* worms. The *dgk-1* gene encodes a diacylglycerol (DAG) kinase,[52] which decreases DAG level by converting it to phosphatidic acid (PA).[53-55] Therefore, DAG signaling is increased in *dgk-1* mutants. DGK-1 was not important for the bordering behavior of control worms that did not experience hypoxia (Figure 6D). However, the *dgk-1* mutation significantly decreased the bordering recovery of *glb-5(+); npr-1(−)* worms after hypoxia. Together, these results suggest that excess of DAG attenuates the recovery of bordering behavior after hypoxia. Moreover, this inhibitory effect is specific to the recovery period and does not apply to worms that were not exposed to hypoxia.

3.8 | PITP-1 effect on aldicarb resistance

So far, our results are consistent with a working model in which PITP-1 restricts PKC-1 activity during the recovery of worms from hypoxia by limiting DAG availability. Previous studies show that increased PKC-1 activity and exogenous PMA sensitize worms to the paralytic effect of the acetylcholinesterase inhibitor aldicarb.[51,56,57] Therefore, we hypothesized that *pitp-1* loss-of-function would result in increased sensitivity of worms to aldicarb after hypoxia. To test this, we measured aldicarb-induced paralysis in *npr-1(−)*, *glb-5(+); npr-1(−)*, and *pitp-1(−); glb-5(+); npr-1(−)* worms after exposure to hypoxia or in worms that were not exposed to hypoxia (as a control). *pitp-1(−); glb-5(+); npr-1(−)* worms were significantly more sensitive to aldicarb than *glb-5(+); npr-1(−)* worms in both experimental conditions (Figure 6E, $P = .0020$, and $P = .0008$, after hypoxia and control conditions, respectively), suggesting that *pitp-1* is generally important for restricting neurotransmission in *C elegans*. Moreover, *npr-1(−)* worms were significantly more sensitive to aldicarb than *glb-5(+); npr-1(−)* animals ($P < .0001$ for both experimental conditions). Notably, the exposure to hypoxia increased the aldicarb resistant of the three strain; Hazard ratios (after 24 hours exposure to hypoxia vs controls) were *npr-1(−)* [0.4564]; *glb-5(+); npr-1(−)* [0.4095]; and *pitp-1(−); glb-5(+); npr-1(−)* [0.3958], suggesting that

hypoxia attenuates neurotransmitter release in a *glb-5* and *pitp-1* independent manner.

Our data suggest that PITP-1 acts in *mod-1*-expressing neurons to facilitate the fast recovery of bordering after hypoxia (Figure 5). Therefore, we hypothesized that restoring *pitp-1* function in these neurons would rescue *pitp-1(−); glb-5(+); npr-1(−)* worms from the hypersensitivity to aldicarb. To test this, we repeated the above aldicarb experiments with transgenic *Pmod-1::pitp-1(cDNA)* worms (these worms display rescued bordering phenotype after hypoxia, Figure 5). As predicted, *Pmod-1::pitp-1(cDNA)* animals were significantly more resistant to aldicarb compared with their *pitp-1(−); glb-5(+); npr-1(−)* parental strain, and this was true for both experimental conditions (*i.e.,* after 24 hours at 1% O_2 and in control worms that did not experience hypoxia) (Figure 6F). Intriguingly, the resistance of *Pmod-1::pitp-1(cDNA)* worms to aldicarb was significantly higher than of *glb-5(+); npr-1(−)* animals ($P < .0001$ for 21% O_2-aldicarb assays and $P = .0002$ for the 1% O_2 assays). Since resistance to aldicarb can arise from impaired pre- or postsynaptic activity,[26] the hyper-resistance of transgenic *Pmod-1::pitp-1* worms to aldicarb may reflect the consequence of over-PITP-1 activity in these neurons, which decreases synaptic transmission to a suboptimal level. In conclusion, this set of experiments further supports the hypothesis that PITP-1 facilitates the fast recovery of bordering after hypoxia by restricting neurotransmission in *mod-1*-expressing neurons.

4 | DISCUSSION

4.1 | PITP-1 acts downstream to O_2-sensing neurons to facilitate fast bordering recovery from hypoxia

We previously isolated the *pdl-1(db508)*, *gcy-35(heb1)*, and *gcy-36(heb3)* mutations that suppress the recovery of bordering eating behavior after hypoxia in *glb-5(+); npr-1(−)* worms.[6,10] These mutations directly interfere with the O_2-sensing machinery in the AQR, PQR, and URX neurons. The *pdl-1* mutation prevents the targeting of the soluble guanylate cyclases GCY-35 O_2-sensor to URX endings, while the *gcy-35/gcy-36* mutations make GCY-35 and GCY-36 insensitive to GLB-5. As a result, *pdl-1(db508)*, *gcy-35(heb1)*, and *gcy-36(heb3)* mutants are generally defective for *glb-5*-dependent-O_2 responses. That is, they do not display a robust decrease in speed when shifted from 21% to 17% O_2 and display high URX Ca^{2+} level at 14% and 17% O_2 after hypoxia.[6,10] Notably, the expression of wild-type *pdl-1*, *gcy-35*, and *gcy-36* in the AQR, PQR, and URX neurons of *pdl-1(db508)*, *gcy-35(heb1)*, and *gcy-36(heb3)* mutants, respectively, rescues both the bordering behavior after hypoxia and the slowing response phenotypes, indicating that the activities of these genes in AQR, PQR, and URX are both necessary and sufficient for GLB-5-dependent O_2 responses.

By contrast, *pitp-1* mutants display a robust slowing response when shifted from 21% to 17% O_2 and a sharp drop in URX Ca^{2+} level upon a 21% to 14% O_2 transition, after hypoxia (Figures 2C and 3C, respectively). Moreover, the recovery of bordering behavior after hypoxia cannot be rescued by restoring wild-type PITP-1 activity in AQR, PQR, and URX or even by expressing *pitp-1* under the promoter region of *glb-5* (Figure 2B), which is expressed in additional neurons, including ADF, ASG, and BAG.[30] Together, these results indicate that PITP-1 is not required for the function of GLB-5 in O_2-sensing per se, and suggest that it acts in other neurons to facilitate the fast recovery from hypoxia. In this respect, it is worth emphasizing that our previous studies suggest that the recovery of bordering behavior after hypoxia depends on the desensitization of the URX neurons by GLB-5.[10] The results of this study imply that URX-desensitization is not sufficient for the fast recovery phenotype and that downstream neurosignaling pathways are also required.

Indeed, our results suggest that the recovery process is mediated by PITP-1-dependent neurosignaling in *mod-1*-expressing neurons. Interestingly, some of the *mod-1*-expression neurons are involved in dietary choice behavior in *C. elegans* and have chemical-synapse connections with the GLB-5-expressing neurons. For example, the AIY interneurons, which have chemical synapses with BAG,[58] appear to be important for finding high-quality food in diverse environments[59] and for regulating food-leaving behavior.[60] Moreover, a recent paper suggests that the transcription factor DAF-16 regulates salt avoidance by controlling neurotransmission between ASER, AIA, and AIY[61]; the same neurons in which PITP-1 acts to regulate salt chemotaxis. Intriguingly, DAF-16 regulates the aversive response to pheromone signals,[62] which could be affected by the O_2 concentration that the worm experience[63] and potentially change the attraction/avoidance of worms to food. In the future, it will be exciting to explore whether DAF-16 controls the recovery of bordering behavior after hypoxia and whether it affects the functions of PITP-1 in both salt and recovery from hypoxia responses.

4.2 | PITP-1 functions in salt chemotaxis and recovery of bordering after hypoxia

A previous study by Iino and colleagues showed that PITP-1 acts in the ASEL/R neurons to facilitate salt (NaCl) chemotaxis.[27] Intriguingly, *pitp-1*-loss-of-function did not affect the Ca^{2+} response to salt in ASER, suggesting that PITP-1 is not important for salt sensing per se but rather for neurotransmission from ASER. Indeed, salt-induced Ca^{2+} responses in the AIB interneurons, which are directly connected through

chemical synapses to the ASER neurons, were significantly decreased in *pitp-1* mutants, further supporting the function of PITP-1 in neurotransmission. Our results show that PITP-1 function in the ASEL/R neurons is not important for the fast recovery of bordering behavior after hypoxia (Figure 4A), suggesting that PITP-1 roles in salt chemotaxis and recovery of eating behavior after hypoxia are distinct. In fact, we show that the expression of wild-type *pitp-1* under the promoter region of *mod-1* results in near-to-wild-type recovery of the bordering behavior after hypoxia (Figure 5). Intriguingly, one of the interneurons in which *mod-1* is expressed is AIB (36). In future studies, we will investigate the effect of PITP-1 on O_2-evoked-Ca^{2+} responses (after hypoxia) in AIB and other interneurons that expresses *mod-1* (*e.g.,* AIY).

4.3 | Is PITP-1 the "GLB-5" of *mod-1*-expressing neuron(s)?

Our previous studies suggest a model in which GLB-5 accelerates the recovery of bordering behavior after hypoxia by decreasing the sensitivity of URX neurons to O_2.[10] In this

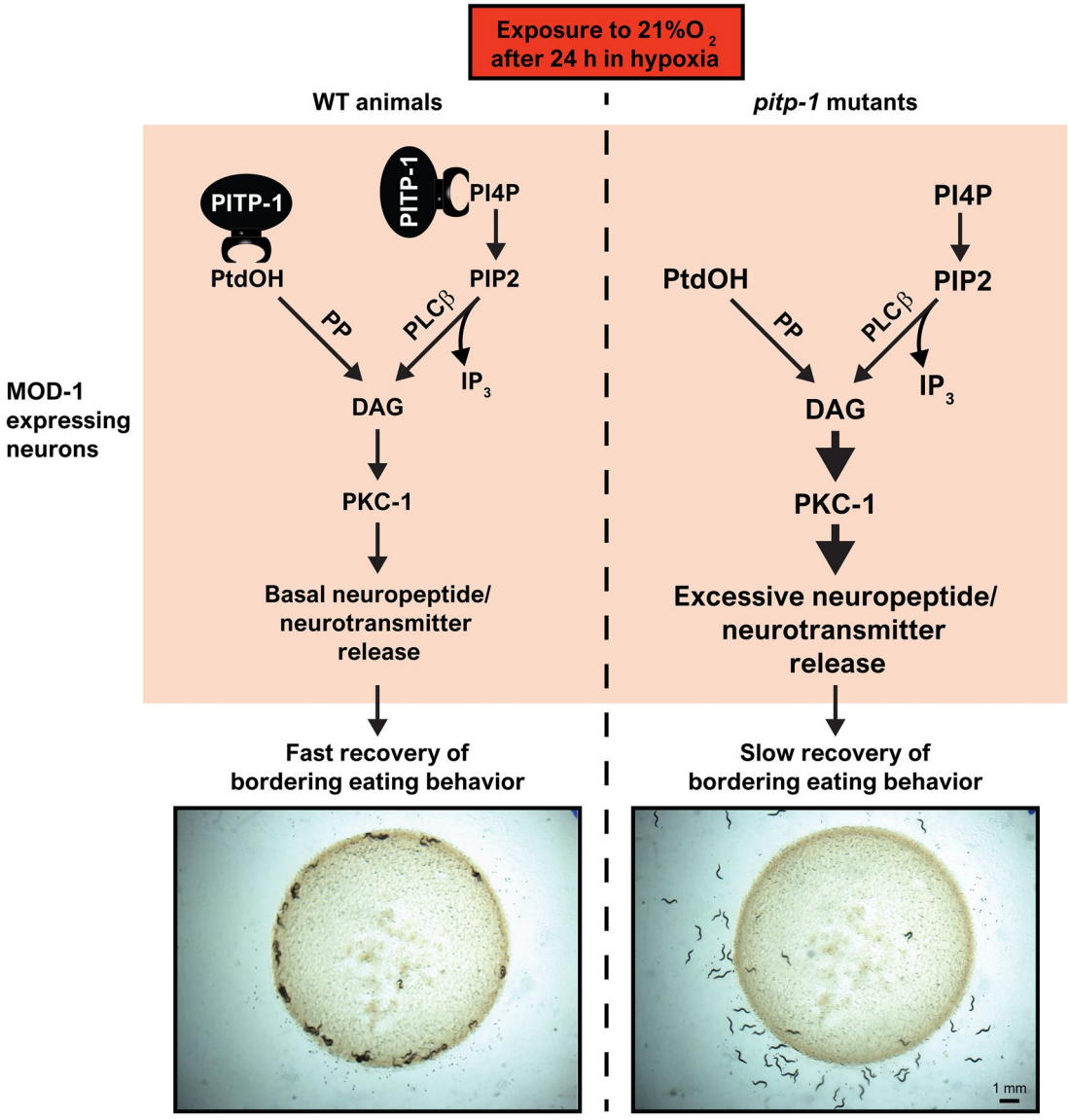

FIGURE 7 An illustrated working model explaining the function of PITP-1 in the *mod-1*-expressing neuron(s) following the exposure of worms to 21% O_2 after 24 hours at 1% O_2. The figure describes the recovery of wild-type (WT) animals (*i.e., glb-5(+);npr-1(−)* worms) vs *pitp-1(−); glb-5(+); npr-1(−)* mutants; left of the dash line are the *mod-1* neurons of WT animals and right of the dash line are the mutant neurons. In WT, PITP-1 inhibits PKC-1 by limiting DAG availability. It does so by limiting PIP2 synthesis and PtdOH dephosphorylation. As a result, PKC-1 is overactivated after hypoxia, a situation that triggers the release of a yet-to-be-identified neurotransmitter(s)/neuropeptide(s), which inhibits the recovery of bordering eating behavior. The larger fonts and arrows, the *pitp-1*-mutants panel, indicate excessive substrate concentration and PKC-1 activity

way, the URX neurons are fine-tuned to respond to subtle changes in the ambient O_2 level. For example, the 21% to ~14% shift that the worm experience when it re-enters the bacterial lawn after leaving it in hypoxia. Here, we would like to extend this model and propose that PITP-1's function in the *mod-1*-expression neurons is analogous to GLB-5 in the O_2-sensing neurons. That is, PITP-1 acts to decrease PKC-1 activity in *mod-1*-expression neurons, and thus, prevent excessive neurotransmission that attenuates the recovery from hypoxia. Below, we present the experimental evidence and logic supporting this working model (Figure 7).

(1) *pkc-1* loss-of-function rescues the recovery phenotype of *pitp-1* mutants (Figure 6A). **(2)** Restoring the activity of wild-type PKC-1 in the *mod-1*-expressing neurons of *pitp-1(−); glb-5(+) pkc-1(−); npr-1(−)* worms attenuates the recovery of bordering behavior after hypoxia (Figure 6A). Moreover, expression of constitutively active PKC-1 in these neurons (*pkc-1(gf)*) significantly inhibits the bordering behavior of the worms (Figure 6B). **(3)** PKC-1 activation increases worms' sensitivity to the acetylcholinesterase inhibitor aldicarb. Indeed, *pitp-1* mutants are more sensitive to aldicarb compared with their parental *glb-5(+); npr-1(−)* strain (Figure 6E). Moreover, rescuing PITP-1 function in the *mod-1*-expression neurons of *pitp-1* mutants increases the resistance to aldicarb (Figure 6F). Together, these observations support the hypothesis that PITP-1 facilitates the fast recovery of bordering after hypoxia by decreasing PKC-1 activity in the *mod-1*-expressing neurons.

PKC-1 is thought to be activated by diacylglycerol (DAG), which can be generated by the following processes: **(a)** Through the cleavage of phosphatidylinositol 4,5-bisphosphate (PIP2) to DAG and inositol 1,4,5-trisphosphate (IP_3) by phospholipase Cβ (PLCβ)[64]; **(b)** Through the dephosphorylation of phosphatidic acid (PtdOH) to DAG by PtdOH phosphatase.[65] The *C. elegans* PITP-1 is a member of the class II phosphatidylinositol transfer proteins, which can control DAG availability by binding & shuttling phosphatidylinositol-4-phosphate (PIP2 precursor[66]) and PtdOH.[66,67] Therefore, we suggest that PITP-1 decreases the activity of PKC-1 by restricting DAG availability.

Two observations support this claim. First, exogenous PMA (DAG analog) decreases the bordering recovery of wild-type *glb-5(+); npr-1(−)* worms after hypoxia (Figure 6C). Second, *dgk-1* loss of function, which increases DAG level, also decreases the recovery of *glb-5(+); npr-1(−)* worms from hypoxia. PKC-1 regulates the secretion of neuropeptides[51] and may function in neurotransmitter release.[50] We hypothesize that excessive secretion of a yet to be identified neuropeptide(s) and/or neurotransmitter(s) inhibit(s) the recovery of bordering behavior after hypoxia.

In this respect it is interesting to mention that amphetamine-induced anorexia in the rat is associated with the expression of several PKC isotypes,[68] including the eta isotype that is structurally similar to the *C. elegans* PKC-1.[69] The anorectic effect is decreased by PKC alpha-antisense knockdown, suggesting that PKC suppresses food consumption.[68] Finally, the amphetamine treatment decreases the level of neuropeptide Y (NPY) mRNA in the rat hypothalamus.[68] This is interesting because NPY is known to regulate food-consumption and is the ligand of the NPY receptor that resembles the *C. elegans* NPR-1, which is also involved in eating-behavior control.[9] In conclusion, despite the significant difference in the complexity of controlling eating behavior between the *C. elegans* worm and the rat and other mammals, we would like to suggest (with due caution) that the link between PKC, neuropeptides, and suppression of eating behavior may be ancient and preserved in evolution. In this context, it would be fascinating to investigate whether orthologs of PITP-1 in the rat are involved in the suppression of eating behavior due to amphetamines and to explore whether mammalian PITP and PKC are involved in high-altitude anorexia.

ACKNOWLEDGMENTS

We thank members of the Gross and Wu laboratories, and G. Kay for critical reading of the manuscript, comments, and advice. We thank the Japan National Bioresource Project for the Nematode *C elegans* and the CGC, which is funded by the National Institutes of Health Office of Research Infrastructure Programs (P40 OD010440), for providing some of the strains. This research was supported by the European Research Council under the European Union's Seventh Framework Program (FP/2007-2013)/ERC Grant Agreement no. 281844, and by the ISRAEL SCIENCE FOUNDATION (grant No. 989/19), the Israel Cancer Association, grant # 20190024.

CONFLICT OF INTEREST

The authors declare that they have no conflict of interest.

AUTHOR CONTRIBUTIONS

Z. Abergel, M. Shaked, V. Shukla, and E. Gross designed and performed the experiments, contributed new reagents, analyzed the data, and wrote the paper; Z.X. Wu Contributed to paper writing; all authors read and approved the final manuscript.

ORCID

Zohar Abergel https://orcid.org/0000-0003-3115-5913

REFERENCES

1. Grimm ER, Steinle NI. Genetics of eating behavior: established and emerging concepts. *Nutr Rev*. 2011;69:52-60.
2. Vats P, Singh SN, Shyam R, et al. Leptin may not be responsible for high altitude anorexia. *High Alt Med Biol*. 2004;5:90-92.
3. Westerterp-Plantenga MS, Westerterp KR, Rubbens M, Verwegen CRT, Richelet JP, Gardette B. Appetite at "high altitude" [Operation Everest III (Comex-'97)]: a simulated ascent of Mount Everest. *J Appl Physiol*. 1999;87:391-399.

4. Farzin M, Albert T, Pierce N, VandenBrooks JM, Dodge T, Harrison JF. Acute and chronic effects of atmospheric oxygen on the feeding behavior of *Drosophila melanogaster* larvae. *J Insect Physiol*. 2014;68:23-29.
5. Van Voorhies WA, Ward S. Broad oxygen tolerance in the nematode *Caenorhabditis elegans*. *J Exp Biol*. 2000;203:2467-2478.
6. Gross E, Soltesz Z, Oda S, Zelmanovich V, Abergel Z, de Bono M. GLOBIN-5-dependent O2 responses are regulated by PDL-1/PrBP that targets prenylated soluble guanylate cyclases to dendritic endings. *J Neurosci*. 2014;34:16726-16738.
7. Cheung BH, Arellano-Carbajal F, Rybicki I, de Bono M. Soluble guanylate cyclases act in neurons exposed to the body fluid to promote *C. elegans* aggregation behavior. *Curr Biol*. 2004;14:1105-1111.
8. Gray JM, Karow DS, Lu H, et al. Oxygen sensation and social feeding mediated by a *C. elegans* guanylate cyclase homologue. *Nature*. 2004;430:317-322.
9. de Bono M, Bargmann CI. Natural variation in a neuropeptide Y receptor homolog modifies social behavior and food response in *C. elegans*. *Cell*. 1998;94:679-689.
10. Abergel Z, Chatterjee AK, Zuckerman B, Gross E. Regulation of neuronal oxygen responses in *C. elegans* is mediated through interactions between globin 5 and the H-NOX domains of soluble guanylate cyclases. *J Neurosci*. 2016;36:963-978.
11. Rogers C, Persson A, Cheung B, de Bono M. Behavioral motifs and neural pathways coordinating O-2 responses and aggregation in *C. elegans*. *Curr Biol*. 2006;16:649-659.
12. Zhao Y, Long L, Xu W, et al. Changes to social feeding behaviors are not sufficient for fitness gains of the *Caenorhabditis elegans* N2 reference strain. *eLife*. 2018;7:e38675.
13. Persson A, Gross E, Laurent P, Busch KE, Bretes H, de Bono M. Natural variation in a neural globin tunes oxygen sensing in wild *Caenorhabditis elegans*. *Nature*. 2009;458:1030-1033.
14. Schmidt M, Gerlach F, Avivi A, et al. Cytoglobin is a respiratory protein in connective tissue and neurons, which is up-regulated by hypoxia. *J Biol Chem*. 2004;279:8063-8069.
15. Burmester T, Weich B, Reinhardt S, Hankeln T. A vertebrate globin expressed in the brain. *Nature*. 2000;407:520-523.
16. Tilleman L, Germani F, De Henau S, et al. Globins in *Caenorhabditis elegans*. *IUBMB Life*. 2011;63:166-174.
17. De Henau S, Braeckman BP. Globin-based redox signaling. *Worm*. 2016;5:e1184390.
18. De Henau S, Tilleman L, Vangheel M, et al. A redox signalling globin is essential for reproduction in *Caenorhabditis elegans*. *Nat Commun*. 2015;6:8782.
19. Sun Y, Jin K, Mao XO, Zhu Y, Greenberg DA. Neuroglobin is up-regulated by and protects neurons from hypoxic-ischemic injury. *Proc Natl Acad Sci U S A*. 2001;98:15306-15311.
20. Kakar S, Hoffman FG, Storz JF, Fabian M, Hargrove MS. Structure and reactivity of hexacoordinate hemoglobins. *Biophys Chem*. 2010;152:1-14.
21. Brenner S. The genetics of *Caenorhabditis elegans*. *Genetics*. 1974;77:71-94.
22. Tomioka M, Adachi T, Suzuki H, Kunitomo H, Schafer WR, Iino Y. The insulin/PI 3-kinase pathway regulates salt chemotaxis learning in *Caenorhabditis elegans*. *Neuron*. 2006;51:613-625.
23. Davis MW, Hammarlund M, Harrach T, Hullett P, Olsen S, Jorgensen EM. Rapid single nucleotide polymorphism mapping in *C. elegans*. *BMC Genom*. 2005;6:118.
24. Green MR, Sambrook J. *Molecular Cloning: A Laboratory Manual*. Cold Spring Harbor Laboratory Press, Cold Spring Harbor, NY, ; 2012.
25. Gibson DG, Young L, Chuang RY, Venter JC, Hutchison CA 3rd, Smith HO. Enzymatic assembly of DNA molecules up to several hundred kilobases. *Nat Methods*. 2009;6:343-345.
26. Mahoney TR, Luo S, Nonet ML. Analysis of synaptic transmission in *Caenorhabditis elegans* using an aldicarb-sensitivity assay. *Nat Protoc*. 2006;1:1772-1777.
27. Iwata R, Oda S, Kunitomo H, Iino Y. Roles for class IIA phosphatidylinositol transfer protein in neurotransmission and behavioral plasticity at the sensory neuron synapses of *Caenorhabditis elegans*. *Proc Natl Acad Sci U S A*. 2011;108:7589-7594.
28. Wormbase. https://www.Wormbase.org/species/c_elegans/gene/WBGene00010813#0123456789abcdef–10
29. Zimmer M, Gray JM, Pokala N, et al. Neurons detect increases and decreases in oxygen levels using distinct guanylate cyclases. *Neuron*. 2009;61:865-879.
30. McGrath PT, Rockman MV, Zimmer M, et al. Quantitative mapping of a digenic behavioral trait implicates globin variation in *C. elegans* sensory behaviors. *Neuron*. 2009;61:692-699.
31. Takeishi A, Yu YXV, Hapiak VM, Bell HW, O'Leary T, Sengupta P. Receptor-type guanylyl cyclases confer thermosensory responses in *C. elegans*. *Neuron*. 2016;90:235-244.
32. Koga M, Ohshima Y. The C. elegans ceh-36 gene encodes a putative homemodomain transcription factor involved in chemosensory functions of ASE and AWC neurons. *J Mol Biol*. 2004;336:579-587.
33. Wojtyniak M, Brear AG, O'Halloran DM, Sengupta P. Cell- and subunit-specific mechanisms of CNG channel ciliary trafficking and localization in *C. elegans*. *J Cell Sci*. 2013;126:4381-4395.
34. Jansen G, Thijssen KL, Werner P, van der Horst M, Hazendonk E, Plasterk RH. The complete family of genes encoding G proteins of *Caenorhabditis elegans*. *Nat Genet*. 1999;21:414-419.
35. Gurel G, Gustafson MA, Pepper JS, Horvitz HR, Koelle MR. Receptors and other signaling proteins required for serotonin control of locomotion in *Caenorhabditis elegans*. *Genetics*. 2012;192:1359-1371.
36. Harris GP, Hapiak VM, Wragg RT, et al. Three distinct amine receptors operating at different levels within the locomotory circuit are each essential for the serotonergic modulation of chemosensation in *Caenorhabditis elegans*. *J Neurosci*. 2009;29:1446-1456.
37. Li Z, Li Y, Yi Y, et al. Dissecting a central flip-flop circuit that integrates contradictory sensory cues in *C. elegans* feeding regulation. *Nat Commun*. 2012;3:776. https://doi.org/10.1038/ncomms1780
38. Tobin DM, Madsen DM, Kahn-Kirby A, et al. Combinatorial expression of TRPV channel proteins defines their sensory functions and subcellular localization in *C. elegans* neurons. *Neuron*. 2002;35:307-318.
39. Tran A, Tang A, O'Loughlin CT, et al. *C. elegans* avoids toxin-producing Streptomyces using a seven transmembrane domain chemosensory receptor. *eLife*. 2017;6:e23770.
40. Coburn CM, Bargmann CI. A putative cyclic nucleotide-gated channel is required for sensory development and function in *C. elegans*. *Neuron*. 1996;17:695-706.
41. Frokjaer-Jensen C, Ailion M, Lockery SR. Ammonium-acetate is sensed by gustatory and olfactory neurons in *Caenorhabditis elegans*. *PLoS ONE*. 2008;3:e2467.

42. Tanizawa Y, Kuhara A, Inada H, Kodama E, Mizuno T, Mori I. Inositol monophosphatase regulates localization of synaptic components and behavior in the mature nervous system of *C. elegans*. *Genes Dev*. 2006;20:3296-3310.
43. Von Stetina SE, Watson JD, Fox RM, et al. Cell-specific microarray profiling experiments reveal a comprehensive picture of gene expression in the *C. elegans* nervous system. *Genome Biol*. 2007;8:R135.
44. Sun CL, Kim E, Crowder CM. Delayed innocent bystander cell death following hypoxia in *Caenorhabditis elegans*. *Cell Death Differ*. 2014;21:557-567.
45. Cai H, Dhondt I, Vandemeulebroucke L, Vlaeminck C, Rasulova M, Braeckman BP. CBP-1 acts in GABAergic neurons to double life span in axenically cultured *Caenorhabditis elegans*. *J Gerontol A Biol Sci Med Sci*. 2019;74:1198-1205.
46. McLntire SL, Jorgensen E, Kaplan J, Horvitz HR. The GABAergic nervous system of *Caenorhabditis elegans*. *Nature*. 1993;364:337-341.
47. Kurland M, O'Meara B, Tucker DK, Ackley BD. The Hox Gene egl-5 acts as a terminal selector for VD13 development via Wnt signaling. *J Dev Biol*. 2020;8:5.
48. Konno Y, Ohno S, Akita Y, Kawasaki H, Suzuki K. Enzymatic properties of a novel phorbol ester receptor/protein kinase, nPKC. *J Biochem*. 1989;106:673-678.
49. Ohno S, Akita Y, Konno Y, Imajoh S, Suzuki K. A novel phorbol ester receptor/protein kinase, nPKC, distantly related to the protein kinase C family. *Cell*. 1988;53:731-741.
50. Hyde R, Corkins ME, Somers GA, Hart AC. PKC-1 acts with the ERK MAPK signaling pathway to regulate *Caenorhabditis elegans* mechanosensory response. *Genes Brain Behav*. 2011;10:286-298.
51. Sieburth D, Madison JM, Kaplan JM. PKC-1 regulates secretion of neuropeptides. *Nat Neurosci*. 2007;10:49-57.
52. Nurrish S, Segalat L, Kaplan JM. Serotonin inhibition of synaptic transmission: Galpha(0) decreases the abundance of UNC-13 at release sites. *Neuron*. 1999;24:231-242.
53. van Blitterswijk WJ, Houssa B. Properties and functions of diacylglycerol kinases. *Cell Signal*. 2000;12:595-605.
54. Luo B, Prescott SM, Topham MK. Diacylglycerol kinase zeta regulates phosphatidylinositol 4-phosphate 5-kinase I alpha by a novel mechanism. *Cell Signal*. 2004;16:891-897.
55. Alam T, Maruyama H, Li C, et al. Axotomy-induced HIF-serotonin signalling axis promotes axon regeneration in *C. elegans*. *Nat Commun*. 2016;7:10388. https://doi.org/10.1038/ncomms10388
56. Nurrish S, Segalat L, Kaplan JM. Serotonin inhibition of synaptic transmission: G alpha(o) decreases the abundance of UNC-13 at release sites. *Neuron*. 1999;24:231-242.
57. Miller KG, Emerson MD, Rand JB. Goalpha and diacylglycerol kinase negatively regulate the Gqalpha pathway in *C. elegans*. *Neuron*. 1999;24:323-333.
58. Altun ZF, Herndon LA, Wolkow CA, Crocker C, Lints R, Hall DH.WormAtlas. 2002– 2018.
59. Shtonda BB, Avery L. Dietary choice behavior in *Caenorhabditis elegans*. *J Exp Biol*. 2006;209:89-102.
60. Milward K, Busch KE, Murphy RJ, de Bono M, Olofsson B. Neuronal and molecular substrates for optimal foraging in Caenorhabditis elegans. *Proc Natl Acad Sci U S A*. 2011;108:20672-20677.
61. Nagashima T, Iino Y, Tomioka M. DAF-16/FOXO promotes taste avoidance learning independently of axonal insulin-like signaling. *PLoS Genet*. 2019;15:e1008297.
62. Park D, Hahm J-H, Park S, et al. A conserved neuronal DAF-16/FoxO plays an important role in conveying pheromone signals to elicit repulsion behavior in *Caenorhabditis elegans*. *Sci Rep*. 2017;7:7260.
63. Fenk LA, de Bono M. Memory of recent oxygen experience switches pheromone valence in Caenorhabditis elegans. *Proc Natl Acad Sci U S A*. 2017;114:4195-4200.
64. Alberts B, Johnson A, Lewis J, Raff M, Roberts K, Walter P. *Molecular Biology of the Cell*. 5th ed. Garland Science, informa Healthcare, Taylor and Francis, New York, NY, ; 2008.
65. Carman GM, Han GS. Phosphatidic acid phosphatase, a key enzyme in the regulation of lipid synthesis. *J Biol Chem*. 2009;284:2593-2597.
66. Grabon A, Bankaitis VA, McDermott MI. The interface between phosphatidylinositol transfer protein function and phosphoinositide signaling in higher eukaryotes. *J Lipid Res*. 2019;60:242-268.
67. Kim S, Kedan A, Marom M, et al. The phosphatidylinositol-transfer protein Nir2 binds phosphatidic acid and positively regulates phosphoinositide signalling. *EMBO Rep*. 2013;14:891-899.
68. Hsieh YS, Yang SF, Chiou HL, Kuo DY. Transcriptional involvement of protein kinase C-alpha isozyme in amphetamine-mediated appetite suppression. *Eur J Neurosci*. 2005;22:715-723.
69. Tabuse Y. Protein kinase C isotypes in *C. elegans*. *J Biochem*. 2002;132:519-522.

SUPPORTING INFORMATION

Additional supporting information may be found online in the Supporting Information section.

How to cite this article: Abergel Z, Shaked M, Shukla V, Wu Z-X, Gross E. The phosphatidylinositol transfer protein PITP-1 facilitates fast recovery of eating behavior after hypoxia in the nematode *Caenorhabditis elegans*. *The FASEB Journal*. 2021;35:e21202. https://doi.org/10.1096/fj.202000704R